

ENHANCED CLASS 8 TRUCK PLATOONING VIA SIMULTANEOUS
SHIFTING AND MODEL PREDICTIVE CONTROL

A Thesis

Submitted to the Faculty

of

Purdue University

by

Ifeoluwa J. Ibitayo

In Partial Fulfillment of the

Requirements for the Degree

of

Master of Science

August 2019

Purdue University

West Lafayette, Indiana

**THE PURDUE UNIVERSITY GRADUATE SCHOOL
STATEMENT OF THESIS APPROVAL**

Dr. Gregory Shaver, Chair

School of Mechanical Engineering

Dr. Peter Meckl

School of Mechanical Engineering

Dr. Steven Son

School of Mechanical Engineering

Approved by:

Dr. Anil Bajaj

Head of the Department of Mechanical Engineering

Dedicated to my family.

ACKNOWLEDGMENTS

I'd like to thank Dr. Shaver for believing in me enough to be my advisor here at Purdue. He's taught me how to be a better communicator, and he's shown a consistent care for my health during my stay here, which as many graduate students know is not always our top priority. I'd like to thank Dr. Jain for providing a lot of feedback and critical insight to my research and my thesis. She's been kind, considerate, and a great help during this process. I'd also like to thank my committee members Dr. Son and Dr. Meckl for giving me feedback on my work.

I'd like to thank the graduate students that mentored me during my time here at Purdue. Alex Taylor taught me how to slow down and gather my thoughts. My mouth can wait for my mind to catch up! Cody Allen sacrificed many, many, many hours of his time to explain basic concepts to me in the test cell and sparked many of the ideas that fueled my research. And, I'd like to thank Jonathon Ore for being a good buddy to me at a very low point for me during my graduate career up until now. Thank you for being open to me and allowing me to be open to you.

I'd like to thank Brady Black for being a transparent and reliable friend who spurred me on at many time when I felt like giving up. Thank you for carrying on the torch of the research described in this thesis. I'd also like to thank Shveta Dhamankar for the many laughs she's shared with me during research and outside of it and all the other graduate students along the way that I will hold in my heart including Eli Deneke. Thank you for all the lunches we shared. You definitely widened my palate and always gave me good food for thought, and you stomached (almost) all of my puns without cringing.

I'd like to thank Faith West for providing a blessed community of believers for me to live with and love on. For the board games, great conversations, and opportunities to serve, I am grateful.

I'd like to thank my parents who have supported me through this crazy adventure, my older brother who has encouraged me along the way, and my little brother who claimed that "I'd rise all the way to the top."

Lastly, I'd like to thank God because He did it.

TABLE OF CONTENTS

	Page
LIST OF TABLES	viii
LIST OF FIGURES	ix
SYMBOLS	xii
ABBREVIATIONS	xiv
ABSTRACT	xv
1 INTRODUCTION	1
1.1 Motivation	1
1.2 Literature Review	3
1.3 Contributions	5
1.4 Thesis Outline	5
2 BACKGROUND	7
2.1 Areas of Fuel Consumption Improvement for Class 8 Trucks	7
2.2 Model Predictive Control	10
3 PLATOONING VIA SIMULTANEOUS SHIFTING	12
3.1 Introduction	12
3.2 Simulation Framework and Implementation of Simultaneous Shifting	12
3.3 Westbound I-74 in Indiana (Moderate Grade)	18
3.4 Northbound I-69 in Indiana (Heavy Grade)	21
3.5 Fuel Consumption Comparison	24
3.6 Summary	26
4 MPC APPLIED TO TRACKING IN A PLATOON	27
4.1 Introduction	27
4.2 Tracking MPC Framework and Algorithm Design	28
4.3 Westbound I-74 in Indiana (Moderate Grade)	33

	Page
4.4 Northbound I-69 in Indiana (Heavy Grade)	35
4.5 Fuel Consumption Comparison	39
4.6 Summary	41
5 ROUTE OPTIMIZED GAP GROWTH TO MINIMIZE FUEL CONSUMPTION	42
5.1 Introduction	42
5.2 Route Optimized Gap Growth Framework and Algorithm Design	42
5.3 Tracking MPC Framework and Algorithm Design	47
5.4 Westbound I-74 in Indiana (Moderate Grade)	49
5.5 Northbound I-69 in Indiana (Heavy Grade)	55
5.6 Summary	61
6 SUMMARY AND FUTURE WORK	62
7 OTHER CONTRIBUTIONS	64
REFERENCES	67

LIST OF TABLES

Table	Page
3.1 Tracking metrics comparison with and without simultaneous shifting on I-74.	19
3.2 Tracking metrics comparison with and without simultaneous shifting on I-69.	22
3.3 Fuel consumption comparison with and without simultaneous shifting on I-74.	25
3.4 Fuel consumption comparison with and without simultaneous shifting on I-69.	26
4.1 Tracking metrics comparison between a production-intent controller and MPC on I-74.	34
4.2 Tracking metrics comparison between a production-intent controller and MPC on I-69.	35
4.3 Tracking metrics comparison between a production-intent controller and MPC with and without simultaneous shifting on I-69.	39
4.4 Fuel consumption comparison between a production-intent controller and MPC on I-74 and a production-intent controller and MPC with and without simultaneous shifting on I-69.	40
5.1 Fuel consumption comparison between a production-intent controller and ROGG up to 40 meters on I-74.	51
5.2 Fuel consumption comparison between a production-intent controller and ROGG up to 40 meters, 30 meters, and 25 meters on I-74.	52
5.3 Fuel consumption comparison between a production-intent controller and ROGG up to 40 meters on I-69.	57
5.4 Fuel consumption comparison between a production-intent controller and ROGG up to 40 meters, 30 meters, and 25 meters on I-69.	59

LIST OF FIGURES

Figure	Page
1.1 The average annual miles traveled for various vehicle categories. [1]	1
1.2 The average annual fuel consumption for various vehicle categories. [1] . . .	2
1.3 Projected increase in freight flow through Indiana from 2011 to 2040 [2]. . .	3
2.1 Platooning reduces air eddying behind the lead truck in a platoon and displaces air in front of the follow truck [25].	9
2.2 The coarsely discretized offline optimization computes an optimal control sequence ($u_{offline}^*$); this information is made available to the online MPC strategy, which computes an optimal control sequence (u_{MPC}^*) over a finer grid. v denotes the velocity trajectory of the vehicle. [24].	9
2.3 A prediction of the future behavior of the plant model is used to optimize the desired control inputs to achieve a control objective. This process is repeated at each time instance to introduce feedback into the system [26]. [27]	10
3.1 I-74 is a representative trucking route in Indiana. Dash cam picture of I-74 (a). I-74 on Indiana state map (b). Zoom-in of I-74 on Indiana state map (c).	13
3.2 A VectorNav VN-200, a type of IMU, was used to obtain grade data for the simulated routes.	13
3.3 Traffic speed data for westbound I-74 at 5 PM on a typical Friday was obtained from INDOT. The color of a bar specifies the average traffic speed, and the height of the bar specifies the percentage of an hour spent at that speed [2].	14
3.4 Traffic speed data for westbound I-74 at 5 PM on a typical Friday was obtained from INDOT (a) and time aligned with grade data for the route (b). The reference speed and grade as a function of time describe the route from a simulation standpoint.	15
3.5 Traffic speed data for northbound I-69 at 5 PM on a typical Friday was obtained from INDOT (a) and time aligned with grade data for the route (b). The reference speed and grade as a function of time describe the route from a simulation standpoint.	16

Figure	Page
3.6 The lead truck is controlled by a driver model, and the follow truck is controlled by either a production-intent platooning controller or a MPC controller.	17
3.7 A free-body diagram of forces acting on a class 8 truck.	17
3.8 The normalized drag coefficients for the lead truck and follow truck as a function of truck separation.	18
3.9 A comparison of the tracking performance of a production-intent controller with and without simultaneous shifting over I-74.	19
3.10 Elevation in meters (a), gear number (b), engine torque in Newton-meters (c), relative velocity in meters per second (d), and truck separation in meters (e) is shown over I-74 between 95 and 145 seconds.	20
3.11 A comparison of truck separation and negative relative velocity with and without simultaneous shifting over I-74.	21
3.12 A comparison of the tracking performance of a production-intent controller with and without simultaneous shifting over I-69.	22
3.13 Elevation in meters (a), gear number (b), engine torque in Newton-meters (c), relative velocity in meters per second (d), and truck separation in meters (e) is shown over I-69 between 1620 and 1740 seconds.	23
3.14 A comparison of truck separation and negative relative velocity with and without simultaneous shifting over I-69.	24
4.1 Constant velocity data for westbound I-74 (a) time aligned with grade data for the route (b).	27
4.2 Constant velocity data for northbound I-69 (a) time aligned with grade data for the route (b).	28
4.3 A free-body diagram of forces acting on a class 8 truck.	29
4.4 A comparison of truck separation in meters (a), torque in Newton-meters (b), and gear number (c) between a production-intent controller and MPC over I-74.	34
4.5 A comparison of truck separation in meters (a), torque in Newton-meters (b), and gear number (c) between a production-intent controller and MPC over I-69.	36
4.6 Elevation in meters (a), gear number (b), engine torque in Newton-meters (c), relative velocity in meters per second (d), and truck separation in meters (e) is shown over I-69 between 200 and 280 seconds.	37

Figure	Page
4.7 A comparison of truck separation in meters (a), torque in Newton-meters (b), and gear number (c) between a production-intent controller and MPC with and without simultaneous shifting over I-69.	38
5.1 A free-body diagram of forces acting on a class 8 truck.	43
5.2 Diagram of Route Optimized Gap Growth implementation	48
5.3 Constant velocity data for westbound I-74 (a) time aligned with grade data for the route (b).	49
5.4 Comparison of desired truck separation and actual truck separation over I-74.	50
5.5 Comparison of truck separation (a) and torque (b) for a production-intent controller and ROGG up to 40 meters over I-74.	51
5.6 Comparison of truck separation (a) and torque (b) for a production-intent controller and ROGG up to 40 meters, 30 meters, and 25 meters over I-74.	53
5.7 Comparison of fuel savings for the follow truck as a function of maximum allowed truck separation for ROGG and a production-intent controller with a set point of 16.7 meters.	54
5.8 Grade (a) and standard deviation of 5 km of grade (b) over I-74.	54
5.9 Constant velocity data for northbound I-69 (a) time aligned with grade data for the route (b).	55
5.10 Comparison of desired truck separation and actual truck separation over I-69.	56
5.11 Comparison of truck separation (a) and torque (b) for a production-intent controller and ROGG up to 40 meters over I-69.	57
5.12 Comparison of truck separation (a) and torque (b) for a production-intent controller and ROGG up to 40 meters, 30 meters, and 25 meters over I-69.	58
5.13 Grade (a) and standard deviation of 5 km of grade (b) over I-69.	60
5.14 Comparison of fuel savings for the follow truck as a function of maximum allowed truck separation for ROGG and a production-intent controller with a set point of 16.7 meters.	60
7.1 Cummins X15 engine test bed in Herrick Laboratories at Purdue University.	64
7.2 Class 8 trucks representative of the trucks that will be used to verify the algorithms developed for the NEXTCAR project.	65

SYMBOLS

a	lead truck's acceleration
A	state matrix
\bar{A}	frontal area
B	input matrix
B_a	acceleration input matrix
B_θ	grade input matrix
$C_{D,0}$	nominal drag coefficient
d	distance between lead and follow truck
d_{des}	desired truck separation
d_{max}	maximum truck separation
d_{set}	distance set point
f	friction coefficient
F_{brake}	brake force
F_{drag}	drag force
$F_{gravity}$	gravity force
F_{motive}	engine force
F_{roll}	rolling resistance force
g	gravity constant
k	discrete time unit
m	mass
m_e	inertial mass
N	horizon length
P_{brake}	brake power
$P_{b,max}$	maximum brake power

$P_{e,max}$	maximum engine power
$P_{e,min}$	maximum retarder power
P_{motive}	engine power
$\dot{P}_{e,max}$	maximum increase in rate of change of engine power
$\dot{P}_{e,min}$	maximum decrease in rate of change of engine power
\dot{P}_{motive}	rate of change of engine power
p_0	y-intercept of drag coefficient linearization
p_1	slope of drag coefficient linearization
u	input vector
V	velocity of the follow truck
\bar{V}	mean velocity of the follow truck over the route
W_a	terminal cost weighting matrix
W_b	state running cost weighting matrix
W_c	input running cost weighting matrix
x	state vector
Δd	distance between current truck separation and set point
ΔV	relative velocity
ρ	air density
θ	grade
τ_b	brake constant
τ_e	engine constant

ABBREVIATIONS

CAD	Computer-Aided Design
CDA	Cylinder De-Activation
CVT	Continuously Variable Transmission
DP	Dynamic Programming
HIL	Hardware In the Loop
IMU	Inertial Measurement Unit
INDOT	Indiana Department of Transportation
MPC	Model Predictive Control
PI	Proportional-Integral
ROGG	Route Optimized Gap Growth
TCP	Transmission Control Protocol
VVA	Variable Valve Actuation

ABSTRACT

Ibitayo, Ifeoluwa J. MSME, Purdue University, August 2019. Enhanced Class 8 Truck Platooning via Simultaneous Shifting and Model Predictive Control. Major Professor: Gregory Shaver.

Class 8 trucks on average drive the most miles and consume the most fuel of any major vehicle category annually. Indiana specifically is the fifth busiest state for commercial freight traffic and moves \$750 billion dollars of freight annually, and this number is expected to grow by 60% by 2040. Reducing fuel consumption for class 8 trucks would have a significant benefit on business and the proportional decrease in CO_2 would be exceptionally beneficial for the environment.

Platooning is one of the most important strategies for increasing class 8 truck fuel savings. Platooning alone can help trucks save upwards of 7% platoon average fuel savings on flat ground. However, it can be difficult for a platooning controller to maintain a desired truck separation during uncoordinated shifting events. Using a high-fidelity simulation model, it is shown that simultaneous shifting—having the follow truck shift whenever the lead truck shifts (unless shifting would cause its engine to overspeed or underspeed)—decreases maximum truck separation by 24% on a moderately challenging grade route and 40% on a heavy grade route.

Model Predictive Control (MPC) of the follow truck is considered as a means to reduce the distance the follow truck falls behind during uncoordinated shifting events. The result in simulation is a reduction in maximum truck separation of 1% on a moderately challenging grade route and 19% on a heavy grade route. However, simultaneous shifting largely alleviates the need for MPC for the sake of tracking for the follow truck.

A different MPC formulation is considered to dynamically change the desired set point for truck separation for routes through a strategy called Route Optimized Gap Growth (ROGG). The result in simulation is 1% greater fuel savings on a moderately challenging grade route and 7% greater fuel savings on a route with heavy grade for the follow truck.

1. INTRODUCTION

1.1 Motivation

Class 8 trucks on average drive the most miles of any major vehicle category annually, 68,000 miles (110,000 km) as shown in Figure 1.1, and consume the most fuel of any major vehicle category annually, 12,900 Gasoline Gallon Equivalents (50,000 liters) as shown in Figure 1.2, which is nearly \$40,000 dollars spent on fuel alone per truck each year.

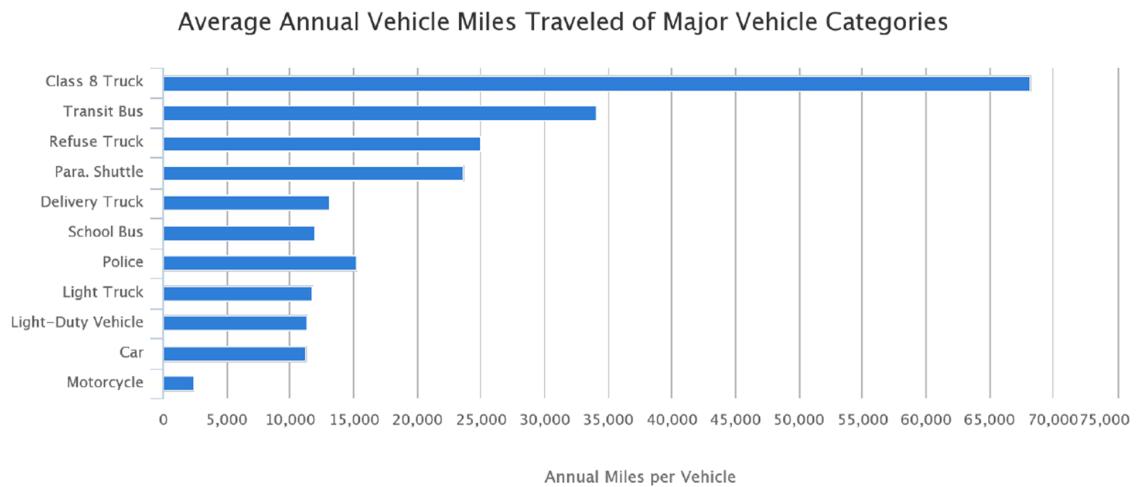


Fig. 1.1. The average annual miles traveled for various vehicle categories. [1]

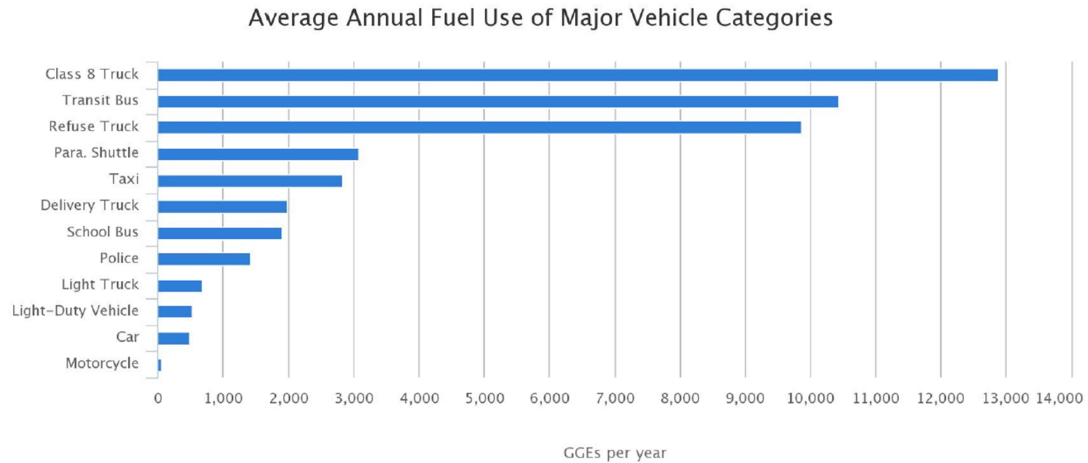


Fig. 1.2. The average annual fuel consumption for various vehicle categories. [1]

The operation of class 8 trucks is especially relevant for Indiana, which moves \$750 billion dollars of freight annually. It is the fifth busiest state for commercial freight traffic, and freight flow is expected to increase by 60% by 2040 as shown in Figure 1.3 [2], so reducing the fuel consumption of the trucks delivering this cargo will be significantly beneficial for local business. Because CO_2 production is proportional to fuel consumption, the correlated reduction in CO_2 will have a significant benefit on the environment as well.

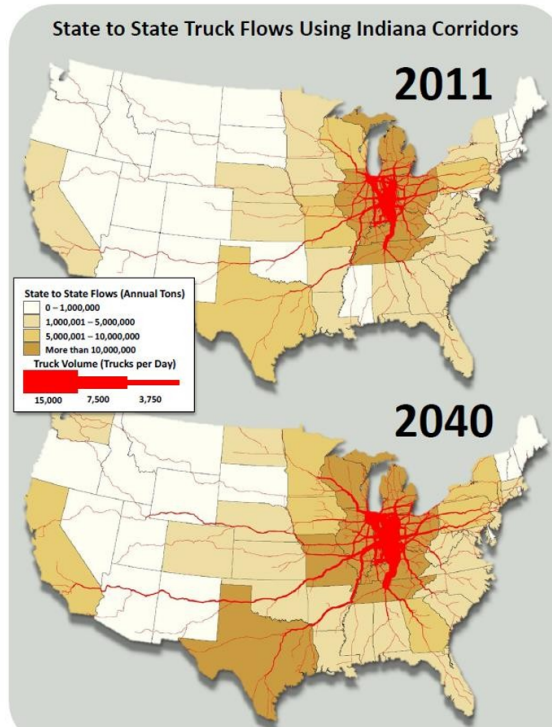


Fig. 1.3. Projected increase in freight flow through Indiana from 2011 to 2040 [2].

1.2 Literature Review

Platooning is the process by which two vehicles travel at very close distances (on the order of tens of meters) for the purpose of reducing drag and is one of the primary areas of research for reducing fuel consumption for semi trucks. Shifting, the process of switching from one gear ratio to another, is an important feature of platooning dynamics because a lack of coordination of shift timing between vehicles in a platoon can cause significant, undesired gap growth; however, it is often neglected completely [3–9], sidestepped by assuming that the vehicles are equipped with Continuously Variable Transmissions (CVTs) [10–14], or modeled but not directly controlled [15].

Shifting dynamics are often neglected to simplify analysis and implementation of platooning controllers [11, 12]. However, neglecting shifting dynamics is not viable because shifting is one of the greatest sources of gap growth when attempting to maintain a desired gap.

Vehicles equipped with CVTs can change gear ratios without discrete shifting events, so their shifting dynamics are far easier to model and control. They are very common in Japanese import sedans and SUVs [16]. However, they are not a plausible simplification for semi trucks because most semi trucks are equipped with transmissions that shift discretely. Discrete shifting events lead to a momentary loss of power as the transmission switches gears, which is the key component of shifting events that leads to truck separation, but this phenomenon is neglected by CVTs.

Lastly, even if shift dynamics are modeled in a simulation framework, they are often not directly controlled because commonly used strategies to command a desired gear number (such as including it as an input in a mixed-integer programming problem) can greatly increase computational cost [17].

A controller is necessary to control the follow vehicle in a platoon to maintain the desired gap throughout a route. A number of instantaneous strategies have been implemented for the sake of tracking and reduced fuel consumption, including optimized Proportional-Integral (PI) controllers by Corona [17] and Alam [6] and an estimated minimum principle controller and a kinetic energy conversion controller by Xu [5], but they do not leverage look-ahead knowledge, which is invaluable for reducing fuel consumption for semi trucks. The upcoming road grade and the lead truck's behavior over a route play a significant role in the achievable fuel savings and cannot be fully accounted for with instantaneous strategies.

One of the most widely used control strategies for platooning vehicles that incorporates look-ahead knowledge is Model Predictive Control (MPC). MPC controllers currently under development are mostly focused on passenger car applications where vehicle mass and road grade do not play nearly as significant a role in fuel consumption [3, 8–10, 12–15, 17] as they do for class 8 trucks. Many of these controllers also neglect platooning drag variation [4, 9, 12, 14, 17] and nearly all of them do not possess high fidelity vehicle models to verify their predicted fuel savings except Santin [15].

1.3 Contributions

The purpose of the research included in this thesis is to utilize shifting strategies and look-ahead knowledge to improve tracking and reduce fuel consumption for semi trucks traveling in a platoon.

As was mentioned earlier, shifting is an important feature of platooning dynamics, and it needs to be coordinated to prevent undesired gap growth. Shifting is included in the simulation model used for analysis in this thesis. The impact of commanding the follow truck to shift at the same as the lead truck (unless shifting will cause the engine to overspeed or underspeed) rather than allowing the transmission controller for the follow truck to shift whenever it desires to will be discussed in this thesis.

MPC was considered in this research for two purposes: Improved tracking and reduced fuel consumption. It was first leveraged for the sake of improved tracking to quantify the benefit of look-ahead knowledge when compared to a production-intent platooning controller by comparing the performance of the production-intent platooning controller to MPC over two representative trucking routes. Another MPC formulation was used to reduce fuel consumption by using look-ahead road grade and the expected lead truck's acceleration over the entire route to determine the optimal truck separation to maximize fuel savings for the follow truck.

1.4 Thesis Outline

This thesis focuses on multiple strategies to improve the follow truck's ability to track the lead truck in a platoon and reduce fuel consumption. This chapter provided the motivation for this thesis and highlights the unique contributions this thesis makes to literature. Chapter 2 provides background on the strategies used to improve fuel consumption for semi trucks. Chapter 3 details the simulation framework and the results obtained with simultaneous shifting. Chapter 4 describes a MPC controller that was used for tracking and the results that were obtained with it. Chapter 5 describes a MPC controller that was used to calculate an optimal truck separation

for a given route and a MPC controller that was used to track the desired truck separation. It also describes the results that were obtained with these controllers. Chapter 6 is a summary of this manuscript and a brief discussion on the next steps for this research. Chapter 7 enumerates the other contributions the author has made to research that are not included in this manuscript.

2. BACKGROUND

2.1 Areas of Fuel Consumption Improvement for Class 8 Trucks

There are three main areas where strategies are being developed to improve fuel consumption for class 8 trucks: engine-level strategies, vehicle-level strategies, and connectivity-enabled strategies. Engine-level strategies focus on reducing pumping losses, increasing thermal efficiency, and/or improving mechanical efficiency. In diesel engines, which many semi trucks are equipped with, pumping losses are the energy that is lost intaking gases and exhausting them. It can be reduced through Variable Valve Actuation (VVA)—which can be used to optimize the opening and closing of valves—and Cylinder De-Activation (CDA)—which reduces the number of cylinders that are pumping fluid [18]. Thermal efficiency can be increased by using higher compression ratios—which result in more complete combustion—and waste heat recovery—which is a strategy to recoup some of the energy lost to heat generation and harness it for useful vehicle operation. Mechanical efficiency can be increased by using more effective lubricants and bearings, reducing the amount of energy lost to friction.

Vehicle-level strategies to reduce fuel consumption focus on improving the drag characteristics of semi trucks by reducing the gap between the tractor and trailer, adding side skirts, and installing boat tails. The goal of all these strategies is to reduce air resistance on the semi truck. When used in combination, they can reduce fuel consumption by over 14% [19].

Lastly, there are connectivity-enabled strategies. Connectivity is the ability of the vehicle to obtain knowledge about the surrounding environment—such as the upcoming weather, road grade, and speed limits—and other vehicles—such as overall traffic flow and the behavior of neighboring vehicles. There are three main applications for connectivity: short-horizon predictive cruise control, long-horizon predictive cruise

control, and platooning. The horizon refers to how far ahead along a route a strategy is applied: Short-horizon is on the order of a few minutes or a few kilometers. Long-horizon is typically applied for an entire route, which can last dozens of minutes or dozens of kilometers. Predictive cruise control optimizes control inputs for a vehicle to minimize fuel consumption over a given horizon. For a short horizon, one of the most common strategies for optimization is Model Predictive Control (MPC), which will be discussed in greater detail in the next section. For long horizon, one of the most common strategies is Dynamic Programming (DP). DP is an algorithmic strategy to reduce a complex problem (such as optimizing fuel consumption over a route with varying traffic and road grade conditions) into simpler, overlapping problems that are solved recursively until an optimal solution is obtained [20]. It has been used by Ozatay [21], Hellstrom [22], and many others [11, 23, 24] for long-horizon predictive cruise control.

Platooning is the process by which two vehicles travel at relatively close inter-vehicular distances for the purpose of reducing drag. The front truck reduces drag for the rear truck by displacing the air it passes through, leaving a hole for the follow truck to drive through. The follow truck reduces drag for the lead truck by reducing air eddies behind it. Air becomes turbulent when it turns around a very sharp corner, which is what occurs when air finishes traveling over the trailer of a semi truck—as shown in Figure 2.1; however, having another truck following very closely behind provides another flat surface for air to travel over when it finishes traveling over the lead truck. The combination of these two phenomena is aerodynamically beneficial for both trucks in the platoon. Platooning is connectivity-enabled because communication is required between both vehicles to prevent accidents and maintain the inter-vehicular distances required for fuel savings.

These connectivity-enabled strategies are non-exclusive. They can be effectively combined, as shown in Figure 2.2 where a coarse, long-horizon, DP-calculated optimal velocity profile is solved before a route is run and fed into an online short-horizon MPC controller that can calculate fine control inputs while the route is being run.

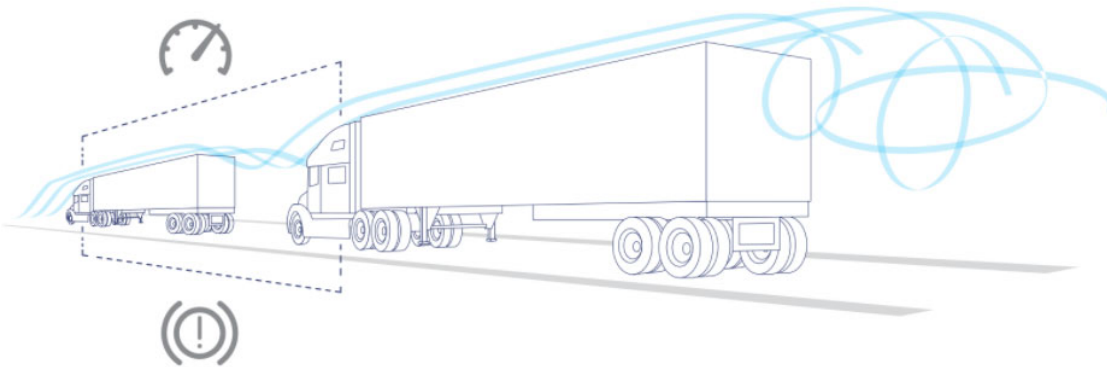


Fig. 2.1. Platooning reduces air eddying behind the lead truck in a platoon and displaces air in front of the follow truck [25].

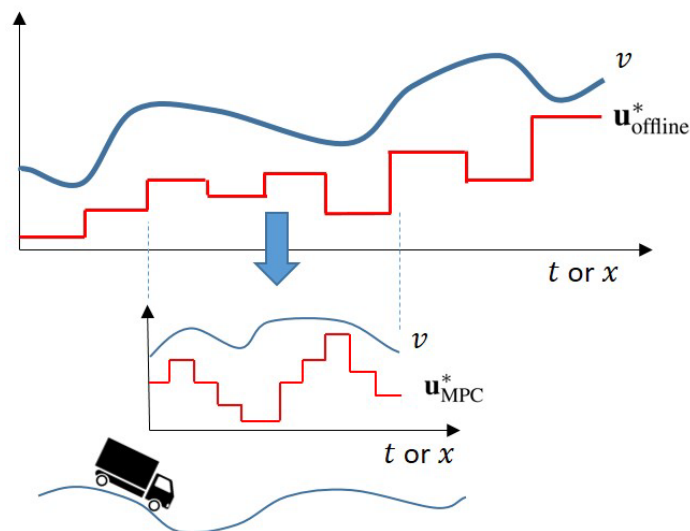


Fig. 2.2. The coarsely discretized offline optimization computes an optimal control sequence ($u_{offline}^*$); this information is made available to the online MPC strategy, which computes an optimal control sequence (u_{MPC}^*) over a finer grid. v denotes the velocity trajectory of the vehicle. [24].

The combination of these connectivity-enabled strategies can sometimes allow even greater fuel savings than they can obtain individually.

Many of the engine-level technologies to reduce fuel consumption are fairly mature. Many vehicle-level technologies, such as side skirts, have become industry standard. Even predictive cruise control has seen commercial applications, such as Cummins' ADEPT technology. However, commercial deployment of platooning for class 8 trucks has been limited and has only begun to gain traction in the trucking industry in the past few years.

2.2 Model Predictive Control

A picture summarizing Model Predictive Control (MPC) is shown in Figure 2.3. First, a system model is developed to predict the future behavior of the plant model. This system model is used to predict the behavior of the plant a certain number of steps into the future. The desired control inputs for the plant are optimized based on this prediction in order to achieve a control objective. The first control input is then implemented, and the process is repeated at the next time instant to introduce feedback into the system [26].

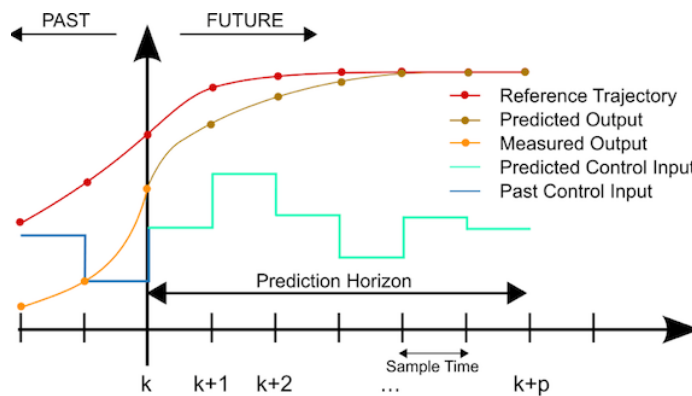


Fig. 2.3. A prediction of the future behavior of the plant model is used to optimize the desired control inputs to achieve a control objective. This process is repeated at each time instance to introduce feedback into the system [26]. [27]

The classical MPC formulation, which is represented in discrete-time, is shown in Equations 2.1-2.4. The system is propagated forward in time via Equation 2.1:

$$x[k + 1] = \mathbf{A}x[k] + \mathbf{B}u[k] \quad (2.1)$$

where x is the state vector, \mathbf{A} is the matrix that relates the evolution of states from one time instance to another, u is the input vector, and \mathbf{B} relates how the inputs affect the states.

This prediction model is provided along with a cost function to minimize and constraints that must be maintained in the solution to the problem as represented in Equations 2.2-2.4:

$$\min J = W_a x[N]^2 + \sum_{k=0}^{N-1} W_b x[k]^2 + W_c u[k]^2 \quad (2.2)$$

$$s.t. \ g(x, u) = 0 \quad (2.3)$$

$$h(x, u) \leq 0 \quad (2.4)$$

where $W_a x[N]^2$ is a terminal cost, $\sum_{k=0}^{N-1} W_b x[k]^2 + W_c u[k]^2$ is a running cost, $g(x, u) = 0$ is an equality constraint, and $h(x, u) \leq 0$ is an inequality constraint.

MPC first began to see traction in commercial applications in the late 70s for use at oil refineries. Chemical processes occur slowly enough to make its application feasible at that time [28]. One of the primary limitations of MPC is its high computational cost. It was not until the 80s that the computational power of computers increased sufficiently to apply MPC to a wider variety of applications [28]. However, it was not until the past ten years that truck platooning became an active area of research, so MPC is only recently being applied to this field.

3. PLATOONING VIA SIMULTANEOUS SHIFTING

3.1 Introduction

Most platooning simulation frameworks to date either model shifting dynamics but do not attempt to optimize shift timing [15], assume the vehicles being studied are equipped with continuous variable transmissions (CVTs) [10–14], or ignore shifting dynamics all together [3–9]. The simulation framework used to analyze strategy performance in this thesis includes shifting dynamics for both a single truck and a two-truck platoon. This chapter analyzes the impact of simultaneous shifting on the performance of a production-intent platooning controller. The performance parameters discussed in this chapter are truck separation, driver comfort, and fuel consumption.

3.2 Simulation Framework and Implementation of Simultaneous Shifting

Westbound I-74 (shown in Figure 3.1) and northbound I-69 are two representative trucking corridors in Indiana and were used for analysis in this thesis. The road grade data for I-74 and I-69 was obtained by integrating the velocity output from a VectorNav VN-200 Inertial Measurement Unit (IMU), which is shown in Figure 3.2. A 150-point moving average filter was used to remove noise due to suspension travel and truck dynamics from the road grade data [29]. The process of obtainment and validation of the grade data used in this paper is described in greater detail by Taylor [29].

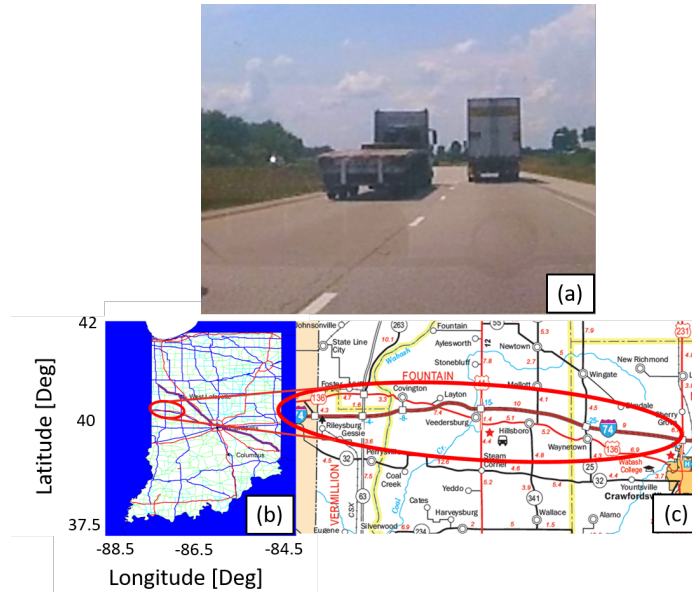


Fig. 3.1. I-74 is a representative trucking route in Indiana. Dash cam picture of I-74 (a). I-74 on Indiana state map (b). Zoom-in of I-74 on Indiana state map (c).

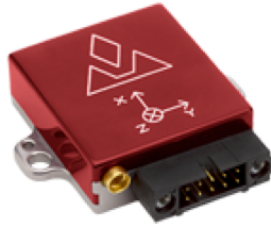


Fig. 3.2. A VectorNav VN-200, a type of IMU, was used to obtain grade data for the simulated routes.

Traffic speed data from the Indiana Department of Transportation (INDOT) was used to generate the reference speed of the lead truck in the platoon for each route. Traffic speed data for westbound I-74 at 5PM on a typical Friday is shown in Figure 3.3. The color of a bar specifies the average traffic speed at the given mile marker, and the height of the bar specifies the percentage of an hour spent at that speed.

The traffic speed data was converted to an average speed at each mile marker. The average speed at each mile marker was then time-aligned with the grade data

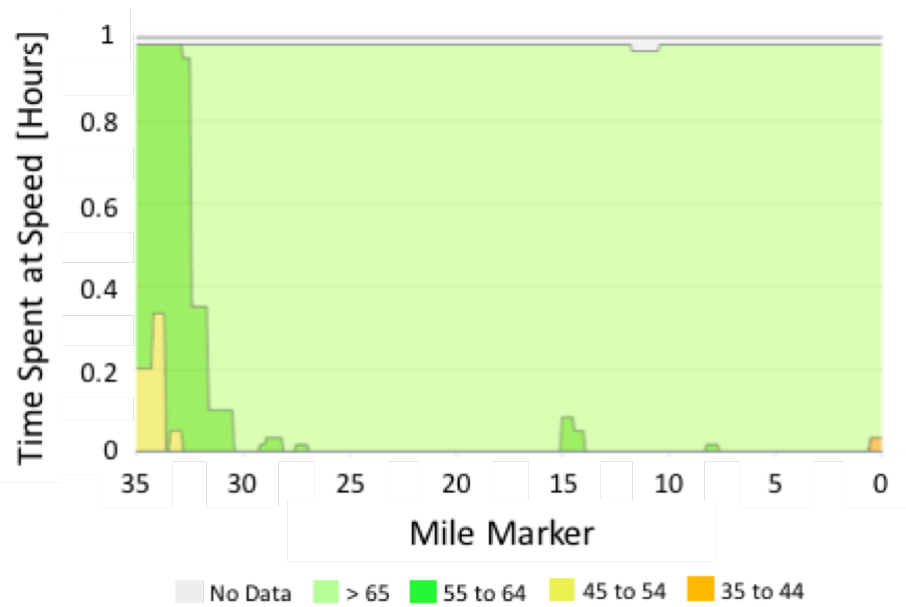


Fig. 3.3. Traffic speed data for westbound I-74 at 5 PM on a typical Friday was obtained from INDOT. The color of a bar specifies the average traffic speed, and the height of the bar specifies the percentage of an hour spent at that speed [2].

calculated for each route. The time-aligned speed and grade data fully describe I-74 and I-69 from a simulation standpoint. The simulated representations of routes I-74 and I-69 are shown in Figures 3.4 and 3.5.

A flow diagram of the platooning simulation framework is shown in Figure 3.6. The modeled lead truck and follow truck (shown in red) were developed by Cummins and are models of Peterbilt 579 class 8 trucks weighing 29,484 kg with Cummins X15 efficiency series engines and Eaton Endurant 12-speed transmissions. The lead truck is controlled by a driver model which commands a desired torque based on the difference between the truck's current velocity and the reference velocity. The follow truck is commanded by either a production-intent platooning controller or a Model Predictive Control (MPC) controller. The details of how the production-intent controller works are confidential, but it takes inputs from both the lead and the follow

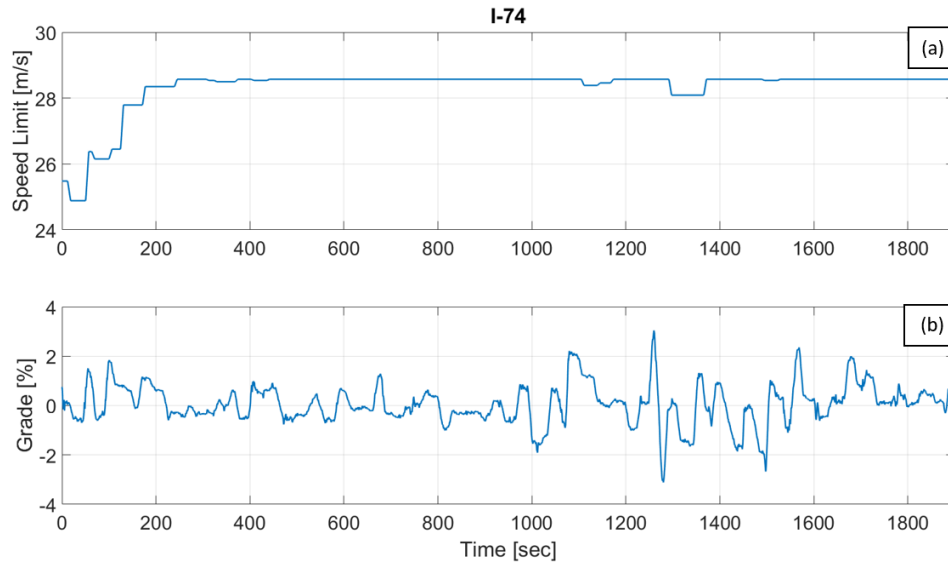


Fig. 3.4. Traffic speed data for westbound I-74 at 5 PM on a typical Friday was obtained from INDOT (a) and time aligned with grade data for the route (b). The reference speed and grade as a function of time describe the route from a simulation standpoint.

truck to generate a desired engine torque and brake acceleration for the follow truck. The details of how the MPC controller works will be discussed in the next chapter.

The forces captured in the simulation framework are shown in Figure 3.7. Forces resulting from engine torque, grade, aerodynamic drag, rolling resistance, and braking are included.

The aerodynamic drag coefficient varies as a function of truck separation for both the lead and the follow truck in correspondence with the experimental data obtained by Salari [30] shown in Figure 3.8. Experimental data obtained by Roeth and Switkes demonstrated that fuel consumption can be reduced by over 7% for a platoon on flat ground because of the reduction in drag for both vehicles [31], so it is essential that the variation of drag as a function of truck separation is captured in the simulation framework.

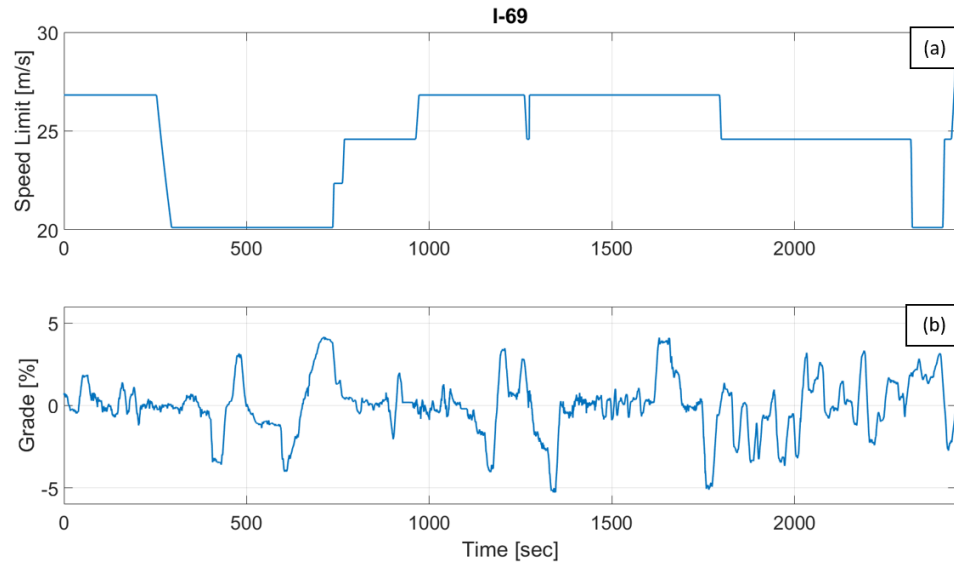


Fig. 3.5. Traffic speed data for northbound I-69 at 5 PM on a typical Friday was obtained from INDOT (a) and time aligned with grade data for the route (b). The reference speed and grade as a function of time describe the route from a simulation standpoint.

The transmission can automatically choose the optimal gear for the truck to be in to conserve fuel, but the gear number can also be commanded manually. The latter feature was utilized to allow the follow truck to shift whenever the lead truck shifted, unless shifting would cause its engine to overspeed or underspeed. This strategy will be called simultaneous shifting throughout the rest of this thesis.

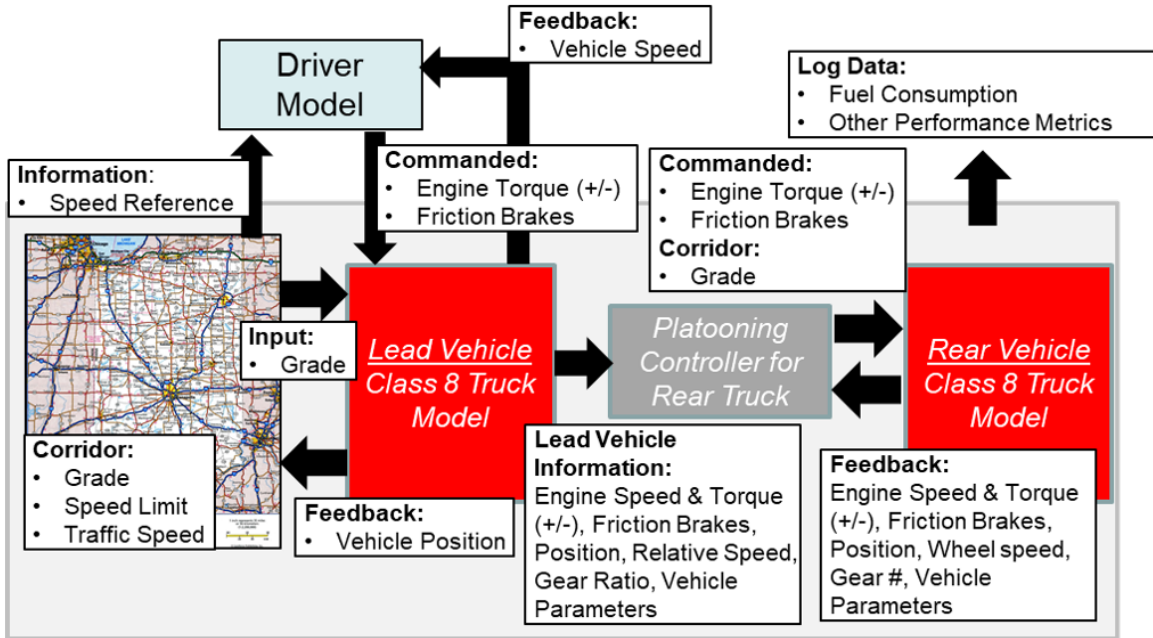


Fig. 3.6. The lead truck is controlled by a driver model, and the follow truck is controlled by either a production-intent platooning controller or a MPC controller.

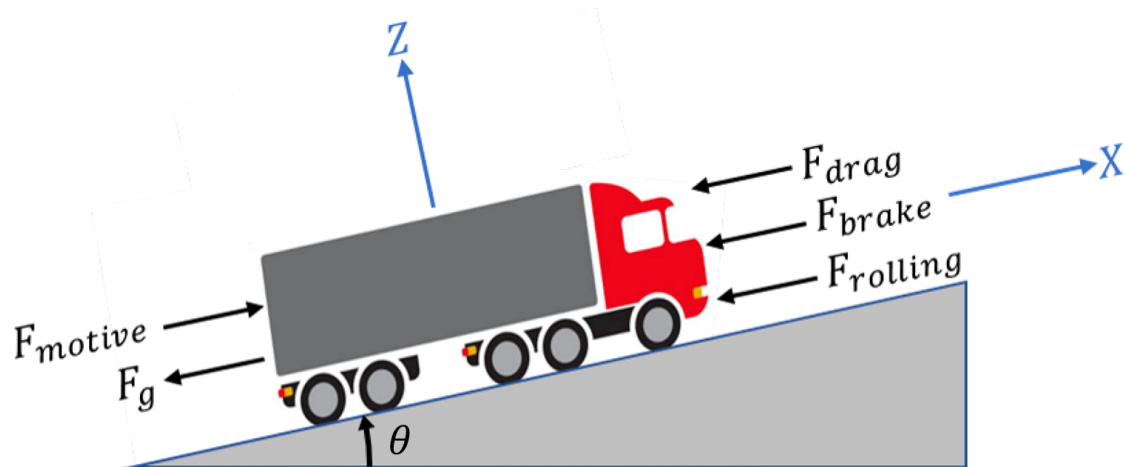


Fig. 3.7. A free-body diagram of forces acting on a class 8 truck.

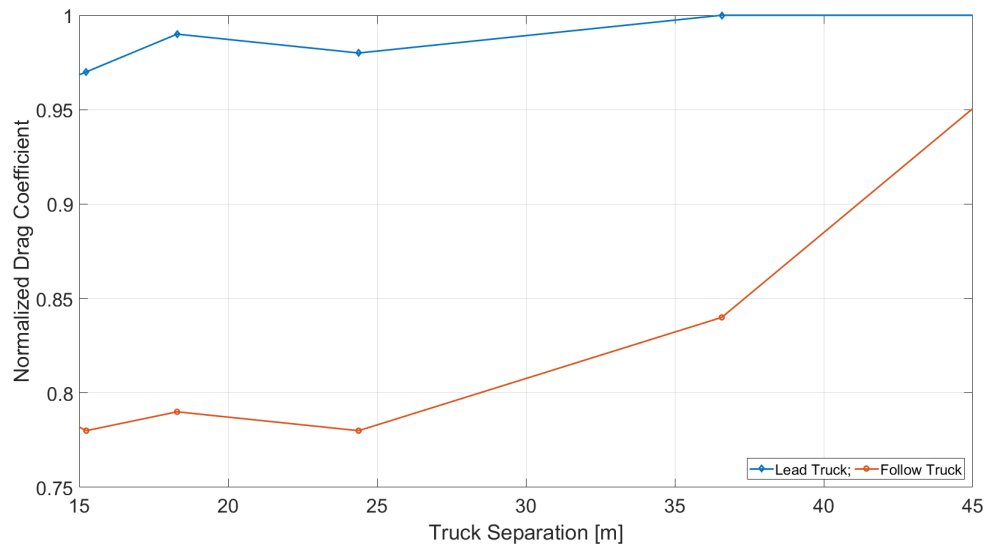


Fig. 3.8. The normalized drag coefficients for the lead truck and follow truck as a function of truck separation.

3.3 Westbound I-74 in Indiana (Moderate Grade)

A comparison of the production-intent controller's tracking performance before and after implementation of simultaneous shifting is shown in Figure 3.9 and Table 3.1 for westbound I-74, which is a moderately challenging grade route. The desired set point was 16.7 meters. The maximum truck separation reached roughly 24 meters on two occasions without simultaneous shifting. With simultaneous shifting, the production-intent controller was able to maintain the truck separation to within two meters of the desired set point.

An explanation for the improved tracking obtained by using simultaneous shifting can be determined by considering Figure 3.10. When the platoon not using simultaneous shifting climbed the sustained uphill (Figure 3.10a), the lead truck downshifted (Figure 3.10b) and maxed out torque (Figure 3.10c), which caused an increase in relative velocity between the lead truck and the follow truck (Figure 3.10d). This

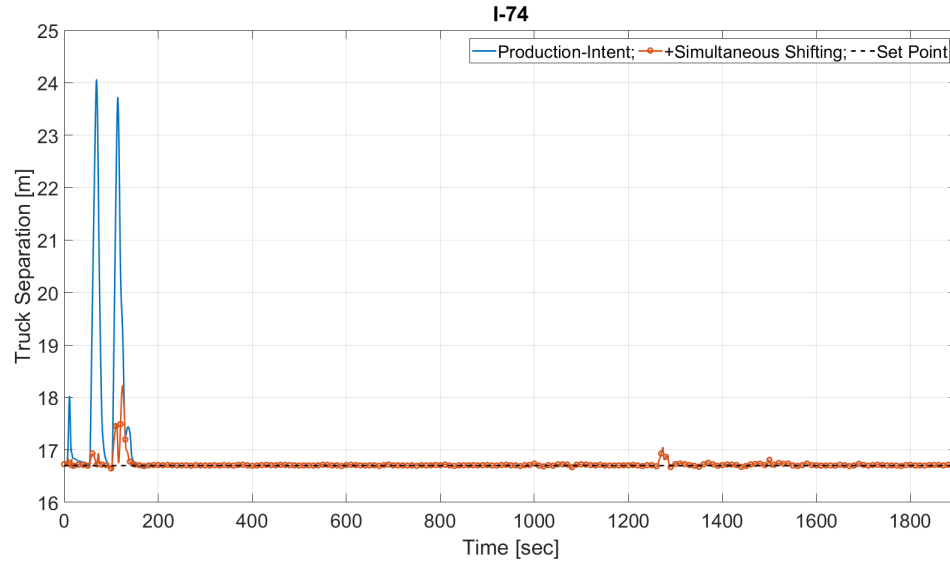


Fig. 3.9. A comparison of the tracking performance of a production-intent controller with and without simultaneous shifting over I-74.

Table 3.1. Tracking metrics comparison with and without simultaneous shifting on I-74.

Strategy over I-74	Average Truck Separation (m)
Production-Intent	16.8
+Simultaneous Shifting	16.7
Strategy over I-74	Maximum Truck Separation (m)
Production-Intent	24.1
+Simultaneous Shifting	18.2

increase in relative velocity was further increased by the follow truck downshifting, which caused it to slow down even more. This increase in relative velocity between

the two-trucks led to an increase in truck separation (Figure 3.10e). However, when the follow truck used simultaneous shifting, it downshifted at the same time as the lead truck; therefore, it was able to maintain the same speed as the lead truck when the lead truck maxed out torque.

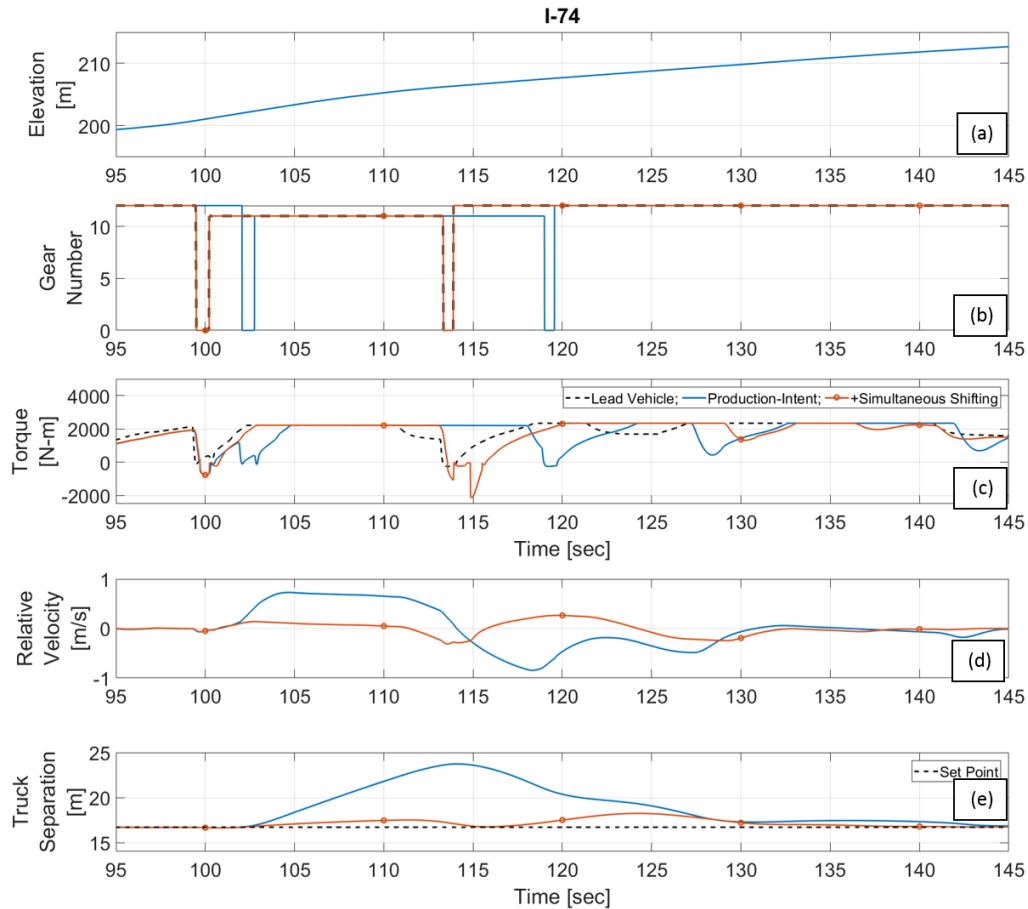


Fig. 3.10. Elevation in meters (a), gear number (b), engine torque in Newton-meters (c), relative velocity in meters per second (d), and truck separation in meters (e) is shown over I-74 between 95 and 145 seconds.

As shown in Figure 3.11, an increase in truck separation caused a significant increase in relative velocity (which is negative when the follow truck is traveling faster than the lead truck) because the follow truck must increase speed to catch

up to the lead truck. Simultaneous shifting improves driver comfort by enabling the production-intent controller to track better, so negative relative velocity remained closer to zero throughout the route.

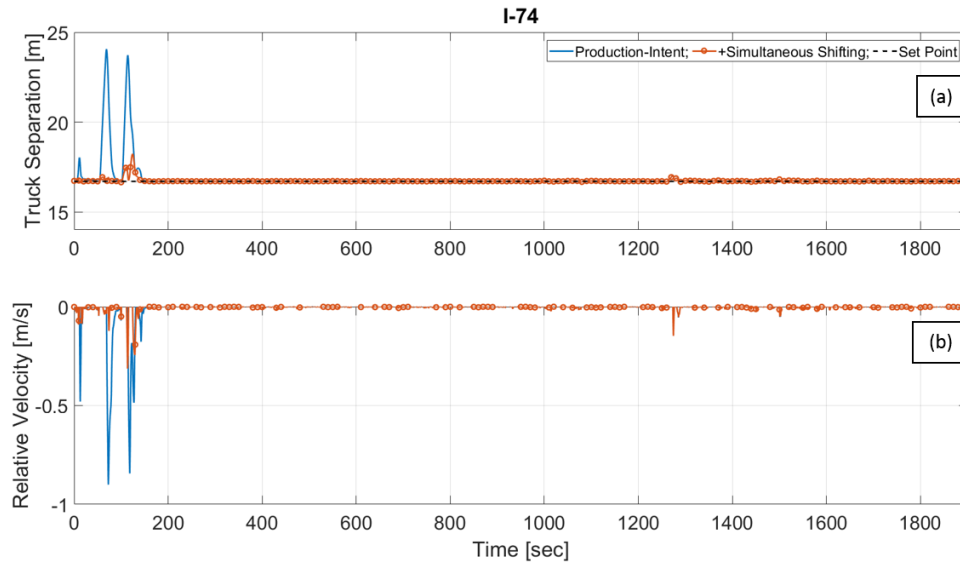


Fig. 3.11. A comparison of truck separation and negative relative velocity with and without simultaneous shifting over I-74.

3.4 Northbound I-69 in Indiana (Heavy Grade)

A comparison of a production-intent controller's tracking performance before and after simultaneous shifting was implemented is shown in Table 3.2 and Figure 3.12 for northbound I-69, which is a more challenging grade route. The desired set point was 16.7 meters. The maximum truck separation exceeded 20 meters several times and even reached double the desired set point on one occasion without simultaneous shifting. With simultaneous shifting, the production-intent controller was able to maintain the truck separation to within four meters of the desired set point.

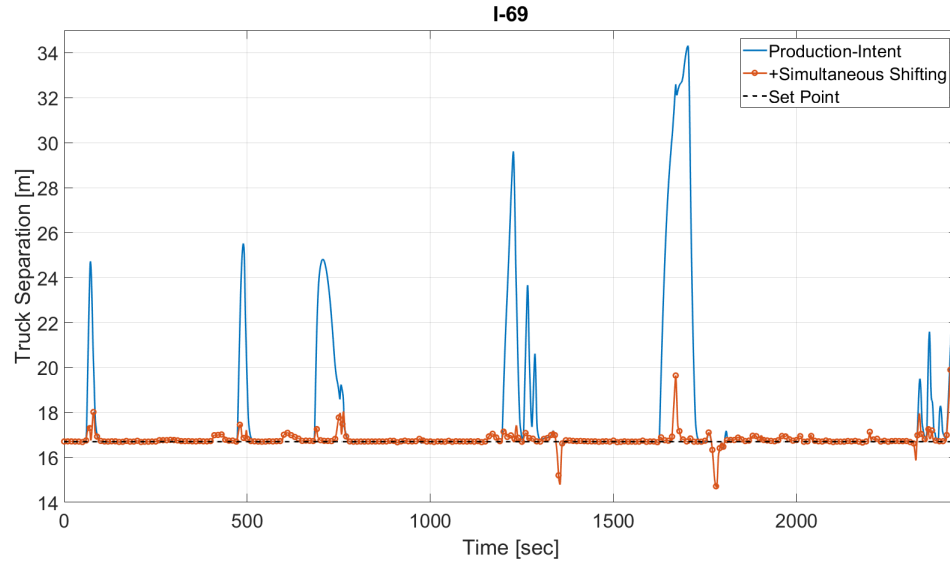


Fig. 3.12. A comparison of the tracking performance of a production-intent controller with and without simultaneous shifting over I-69.

Table 3.2. Tracking metrics comparison with and without simultaneous shifting on I-69.

Strategy over I-69	Average Truck Separation (m)
Production-Intent	17.7
+Simultaneous Shifting	16.8
Strategy over I-69	Maximum Truck Separation (m)
Production-Intent	34.3
+Simultaneous Shifting	20.5

When the platoon climbed the sustained uphill (Figure 3.13a), the lead truck downshifted twice (Figure 3.13b) and maxed out torque (Figure 3.13c), which caused

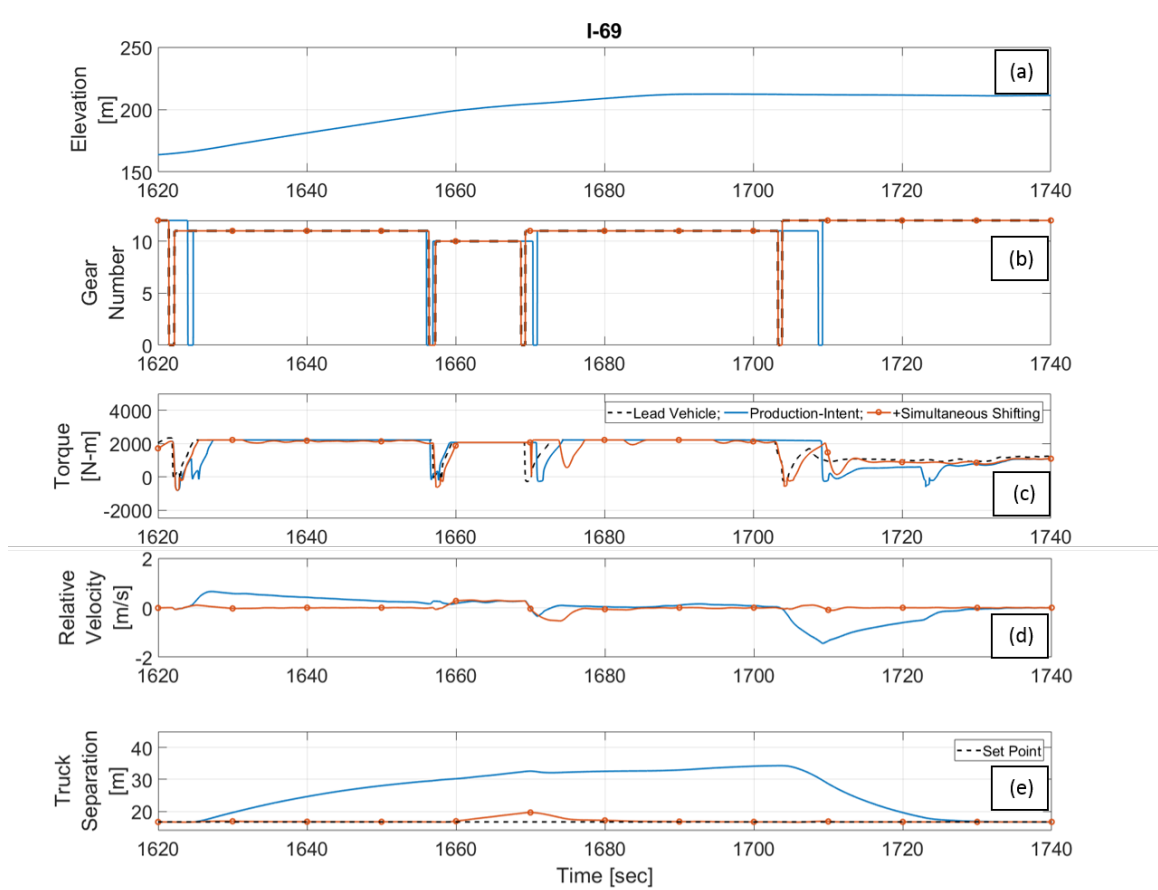


Fig. 3.13. Elevation in meters (a), gear number (b), engine torque in Newton-meters (c), relative velocity in meters per second (d), and truck separation in meters (e) is shown over I-69 between 1620 and 1740 seconds.

an increase in relative velocity between the lead truck and the follow truck (Figure 3.13d). This increase in relative velocity was further increased by the follow truck downshifting, which caused it to slow down even more. This increase in relative velocity between the two-trucks led to an increase in truck separation (Figure 3.13e). However, when the follow truck used simultaneous shifting, it downshifted at the same time as the lead truck; therefore, it was able to maintain the same speed as the lead truck when the lead truck maxes out torque.

As shown in Figure 3.14, the increase in truck separation caused an increase in relative velocity (which is negative when the follow truck is traveling faster than the lead truck). Simultaneous shifting improves driver comfort by enabling the production-intent controller to track better, so even on this heavy grade route, negative relative velocity remained close to zero throughout the route.

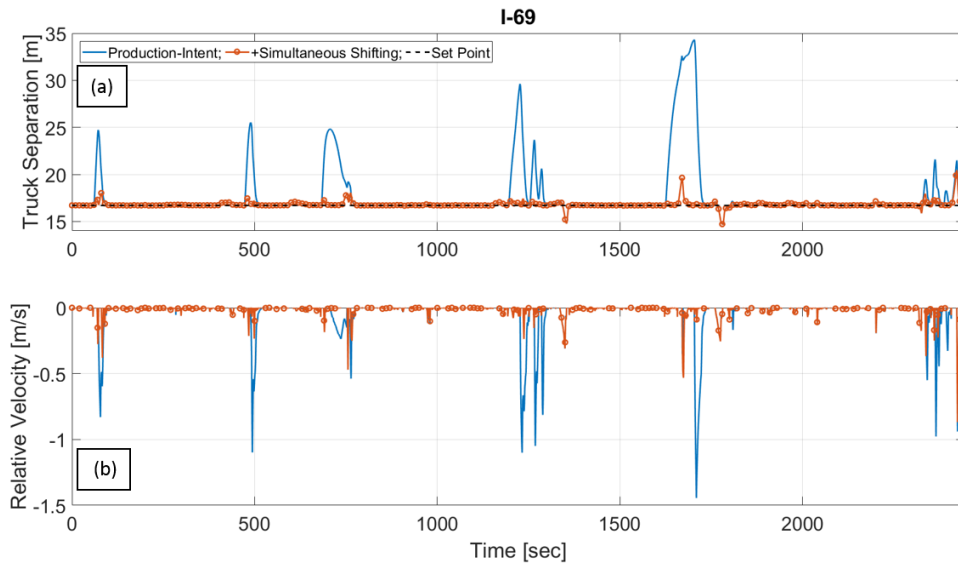


Fig. 3.14. A comparison of truck separation and negative relative velocity with and without simultaneous shifting over I-69.

3.5 Fuel Consumption Comparison

The fuel consumption of the platoon with and without simultaneous shifting was virtually unchanged on both I-74 and I-69, as shown in Tables 3.3 and 3.4. The single truck baseline is the fuel consumed by a single truck traveling over the route and is used as the value by which the various strategies used for platooning are normalized.

Using simultaneous shifting did not significantly affect the fuel consumption of the platoon because the drag coefficient remained nearly unchanged even at the larger

truck separations experienced momentarily over I-74 and I-69, as was shown in Figure 3.8.

Table 3.3. Fuel consumption comparison with and without simultaneous shifting on I-74.

Strategy over I-74	Lead Truck Fuel Consumption
Single truck Baseline	1.0
Production-Intent	0.99
+Simultaneous Shifting	0.99
Strategy over I-74	Follow Truck Fuel Consumption
Single truck Baseline	1.0
Production-Intent	0.89
+Simultaneous Shifting	0.89

Table 3.4. Fuel consumption comparison with and without simultaneous shifting on I-69.

Strategy over I-69	Lead Truck Fuel Consumption
Single Truck Baseline	1.0
Production-Intent	0.99
+Simultaneous Shifting	0.99
Strategy over I-69	Follow Truck Fuel Consumption
Single Truck Baseline	1.0
Production-Intent	0.93
+Simultaneous Shifting	0.93

However, simultaneous shifting is valuable because it improves driver comfort and increases the amount of time that platooning can be implemented, especially on routes with challenging grade.

3.6 Summary

Simultaneous shifting significantly improves tracking and driver comfort over a variety of routes. For a set point of 16.7 meters on I-74, simultaneous shifting reduced the maximum truck separation from 24.1 meters to 18.2 meters. For a set point of 16.7 meters on I-69 (which is a more challenging grade route), the improvement was even more drastic. Simultaneous shifting reduced the maximum truck separation from 34.3 meters to 20.5 meters. Fuel consumption when simultaneous shifting is implemented is unchanged, so its primary fuel savings benefit comes from being able to implement platooning on routes with more challenging grade by significantly improving driver comfort.

4. MPC APPLIED TO TRACKING IN A PLATOON

4.1 Introduction

This chapter considers how much short-horizon look-ahead knowledge of the upcoming grade and the lead truck's acceleration over the route could improve tracking performance. The trucking routes that were used for analysis for this chapter and the next are shown in Figures 4.1 and 4.2.

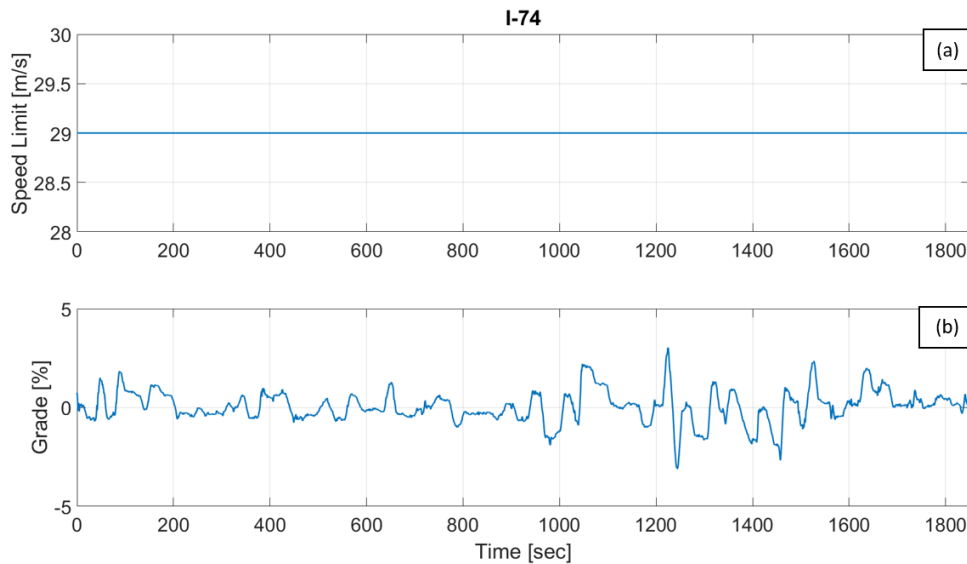


Fig. 4.1. Constant velocity data for westbound I-74 (a) time aligned with grade data for the route (b).

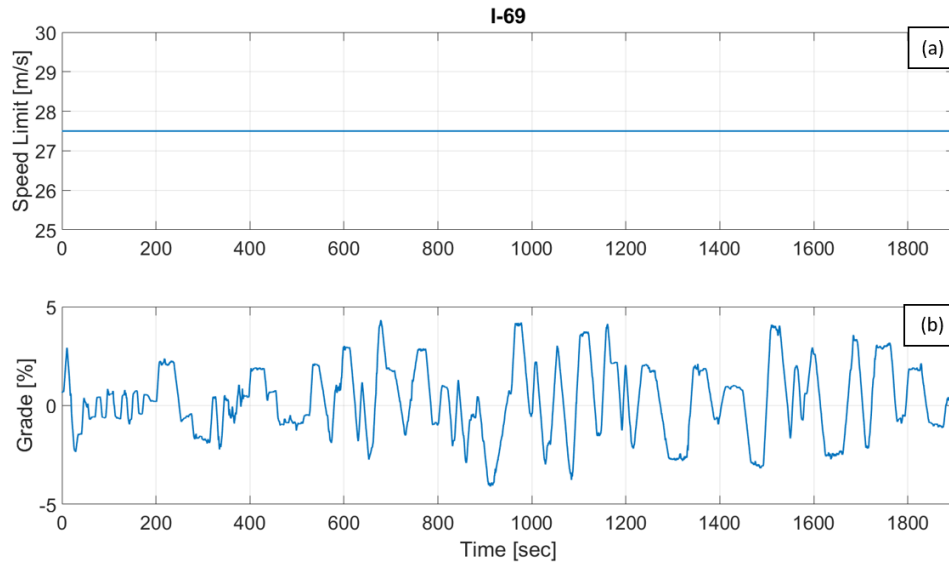


Fig. 4.2. Constant velocity data for northbound I-69 (a) time aligned with grade data for the route (b).

4.2 Tracking MPC Framework and Algorithm Design

A linear model of a class 8 truck following another truck was developed for a Model Predictive Control (MPC) controller. The free body diagram of a class 8 truck shown in Figure 5.1 will be used as a reference for all of the forces on a semi truck.

The motive force on the truck was represented by:

$$F_{motive} = P_e/V \quad (4.1)$$

where P_e is engine power and V is velocity. Power was used because it is independent of gear number allowing the nonlinearities associated with gear shifting to be neglected within the controller. A similar equation was used to represent the brake force:

$$F_{brake} = P_{brake}/V \quad (4.2)$$

where P_{brake} is brake power and V is velocity.

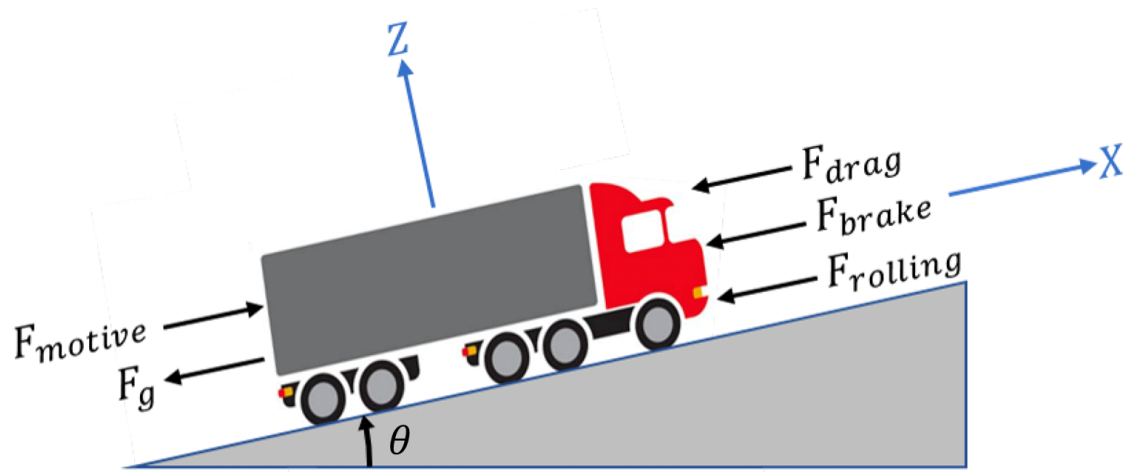


Fig. 4.3. A free-body diagram of forces acting on a class 8 truck.

The force of gravity was represented by:

$$F_{gravity} = mg\theta \quad (4.3)$$

where m is the mass of the truck, g is the gravity constant, and θ is grade. Small angle approximation was used to approximate $\sin(\theta)$ as θ .

The force of rolling resistance was represented by:

$$F_{roll} = mgf \quad (4.4)$$

where m is the mass of the truck, g is the gravity constant, and f is friction coefficient. Small angle approximation was used to approximate $\cos(\theta)$ as 1. The force of drag, which was mentioned earlier as varying with both velocity and truck separation, was represented by:

$$F_{drag} = 1/2\rho\bar{A}C_{D,0}(p_0V\bar{V} + p_1d\bar{V}^2) \quad (4.5)$$

where ρ is the density of air, $C_{D,0}$ is the nominal drag coefficient, V is the current velocity of the follow truck, \bar{V} is the average velocity of the follow truck over the

corridor, d is the distance between the lead truck and the follow truck, p_0 is the y -intercept of the linearization of drag as a function of distance for the follow truck, p_1 is the slope of the linearization of drag as a function of distance for the follow truck. This equation was obtained by linearizing the nonlinear drag variation as a function of truck separation shown in Figure 3.8. Then, a first-order Taylor expansion was applied to the force of drag to obtain its variation as a linear function of both velocity and truck separation.

Along with these forces, three coupling terms were considered: The difference between the trucks' current separation and the distance set point (which is 16.7 meters for platooning), the difference in velocity between the lead truck and the follow truck, and the distance between the lead truck and the follow truck. The difference between the current truck separation and the distance set point will be referred to as Δd in this thesis. The difference between the lead truck's velocity and the follow truck's will be referred to as ΔV . And, the distance between the lead truck and the follow truck will be referred to as d .

The prediction model for the system is shown below:

$$x[k + 1] = \mathbf{A}x[k] + \mathbf{B}u[k] + \mathbf{B}_a a[k] + \mathbf{B}_\theta \theta[k] \quad (4.6)$$

where x is the state vector, \mathbf{A} relates the evolution of states from one time instance to the next, u is the input vector, \mathbf{B} relates how the inputs affect the states, a is the lead vehicle's acceleration, \mathbf{B}_a relates how the lead vehicle's acceleration affects the states, θ is road grade, and \mathbf{B}_θ relates how the road grade affects the states. The acceleration of the lead truck and road grade were treated as disturbances so that they could change dynamically over the MPC horizon.

The state vector is shown below:

$$x = \begin{bmatrix} \Delta d \\ \Delta V \\ V \\ P_e \\ P_b \\ f \\ d \end{bmatrix} \quad (4.7)$$

where Δd is the distance between the platoon's current truck separation and the desired truck separation of 16.7 meters. ΔV is the relative velocity between the lead truck and the follow truck. V is the velocity of the follow truck. P_e is the engine power of the follow truck. P_b is the brake power of the follow truck. f is the friction coefficient. d is the distance between the lead truck and the follow truck.

The state matrix, \mathbf{A} , is shown below:

$$\mathbf{A} = \begin{bmatrix} 0 & 1 & 0 & 0 & 0 & 0 & 0 \\ 0 & 0 & \frac{\rho \bar{A} C_{D,0} \bar{V} p_0}{2m_e} & -\frac{\eta_t}{m_e \bar{V}} & \frac{1}{m_e \bar{V}} & \frac{m}{m_e} g & \frac{\rho \bar{A} C_{D,0} \bar{V}^2 p_1}{2m_e} \\ 0 & 0 & -\frac{\rho \bar{A} C_{D,0} \bar{V} p_0}{2m_e} & \frac{\eta_t}{m_e \bar{V}} & -\frac{1}{m_e \bar{V}} & -\frac{m}{m_e} g & -\frac{\rho \bar{A} C_{D,0} \bar{V}^2 p_1}{2m_e} \\ 0 & 0 & 0 & -\frac{1}{\tau_e} & 0 & 0 & 0 \\ 0 & 0 & 0 & 0 & -\frac{1}{\tau_b} & 0 & 0 \\ 0 & 0 & 0 & 0 & 0 & 0 & 0 \\ 0 & 1 & 0 & 0 & 0 & 0 & 0 \end{bmatrix} \quad (4.8)$$

where ρ is air density, \bar{A} is the frontal area of the semi truck, $C_{D,0}$ is the nominal drag coefficient, \bar{V} is the average velocity of the follow truck over the route, p_0 is the y-intercept of the linearization of drag as a function of distance for the follow truck, m_e is the inertial mass of the semi truck, η_t is the drivetrain efficiency, g is the gravity constant, p_1 is the slope of the linearization of drag as a function of distance for the follow truck, τ_e is the engine time constant, and τ_b is the brake time constant.

The input matrix, \mathbf{B} , is shown below:

$$\mathbf{B} = \begin{bmatrix} 0 & 0 \\ 0 & 0 \\ 0 & 0 \\ \frac{1}{\tau_e} & 0 \\ 0 & \frac{1}{\tau_b} \\ 0 & 0 \\ 0 & 0 \end{bmatrix} \quad (4.9)$$

where τ_e is the engine time constant, and τ_b is the brake time constant.

The acceleration input matrix, \mathbf{B}_a , is shown below:

$$\mathbf{B}_a = \begin{bmatrix} 0 \\ 1 \\ 0 \\ 0 \\ 0 \\ 0 \\ 0 \end{bmatrix} \quad (4.10)$$

The grade input matrix, \mathbf{B}_θ , is shown below:

$$\mathbf{B}_\theta = \begin{bmatrix} 0 \\ \frac{m}{m_e}g \\ -\frac{m}{m_e}g \\ 0 \\ 0 \\ 0 \\ 0 \end{bmatrix} \quad (4.11)$$

where m is the mass of the truck, g is the gravity constant, and m_e is the inertial mass.

The objective and constraints for the MPC problem are shown below:

$$\min J = \sum_{k=0}^{N-1} \Delta d[k]^2 \quad (4.12)$$

$$s.t. P_{e,min} \leq P_e \leq P_{e,max} \quad (4.13)$$

$$\dot{P}_{e,min} \leq \dot{P}_e \leq \dot{P}_{e,max} \quad (4.14)$$

$$0 \leq P_{brake} \leq P_{b,max} \quad (4.15)$$

where Δd is the distance between the current truck separation and the desired truck separation—i.e. tracking error, P_e is engine power, $P_{e,min}$ is maximum retarder (i.e. negative engine) power, $P_{e,max}$ is maximum positive engine power, \dot{P}_e is the rate of change of engine power, $\dot{P}_{e,min}$ is the fastest engine power can decrease, and $\dot{P}_{e,max}$ is the fastest engine power can increase, P_{brake} is brake power, and $P_{b,max}$ is maximum brake power. In short, the objective is to minimize tracking error while maintaining realistic constraints on the engine and brakes.

The controller was applied with a 15-second look-ahead horizon in closed loop with the vehicle models and driver model described in chapter 3.

4.3 Westbound I-74 in Indiana (Moderate Grade)

A comparison of the truck separation, torque, and gear number of the platoon with the follow truck controlled by a production-intent controller and the platoon with the follow truck controlled by MPC is shown in Figure 4.4, and a comparison of the tracking metrics obtained with the follow truck controlled by a production-intent controller and the follow truck controlled by MPC are shown in Table 4.1.

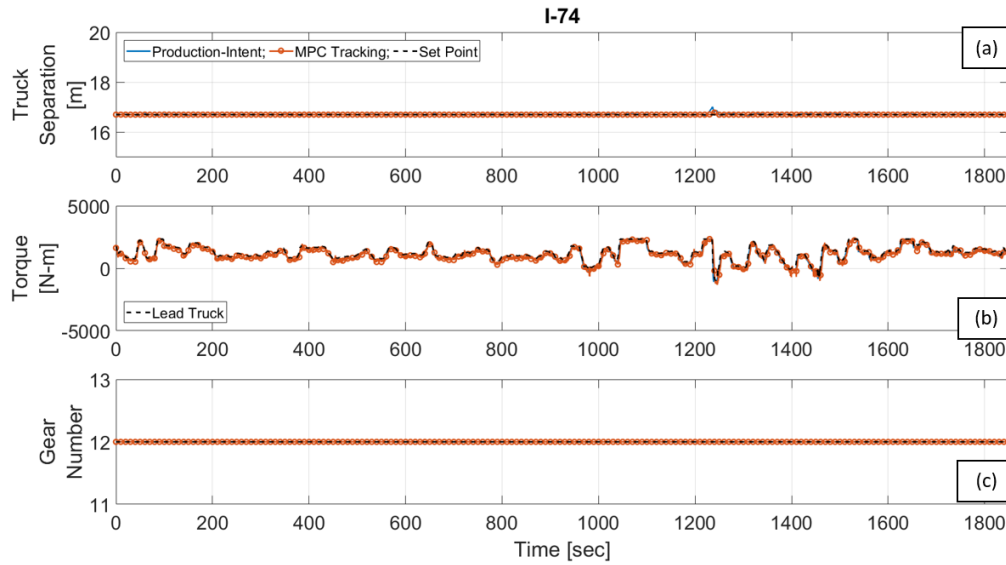


Fig. 4.4. A comparison of truck separation in meters (a), torque in Newton-meters (b), and gear number (c) between a production-intent controller and MPC over I-74.

Table 4.1. Tracking metrics comparison between a production-intent controller and MPC on I-74.

Strategy over I-74	Average Truck Separation (m)
Production-Intent	16.7
MPC	16.7
Strategy over I-74	Maximum Truck Separation (m)
Production-Intent	17.0
MPC	16.8

The follow truck controlled by a production-intent controller was able to effectively track the lead truck when attempting to maintain a constant velocity over the moderate grade route. This route functioned as an effective baseline to demonstrate that look-ahead knowledge would not adversely affect performance on a route with moderately challenging grade variation.

4.4 Northbound I-69 in Indiana (Heavy Grade)

A production-intent controller and MPC were each used as the controller for the follow truck while platooning over I-69, which is a more challenging grade route. A comparison of the truck separation, torque, and gear number of the platoon with the follow truck controlled by a production-intent controller and the platoon with the follow truck controlled by MPC is shown in Figure 4.5, and a comparison of the tracking metrics obtained with the follow truck controlled by a production-intent controller and the follow truck controlled by MPC over I-69 are shown in Table 4.2.

Table 4.2. Tracking metrics comparison between a production-intent controller and MPC on I-69.

Strategy over I-69	Average Truck Separation (m)
Production-Intent	19.4
MPC	18.5
Strategy over I-69	Maximum Truck Separation (m)
Production-Intent	35.8
MPC	29.0

On this more challenging grade route, the production-intent controller struggled to maintain the desired truck separation of 16.7 meters at numerous instances in time.

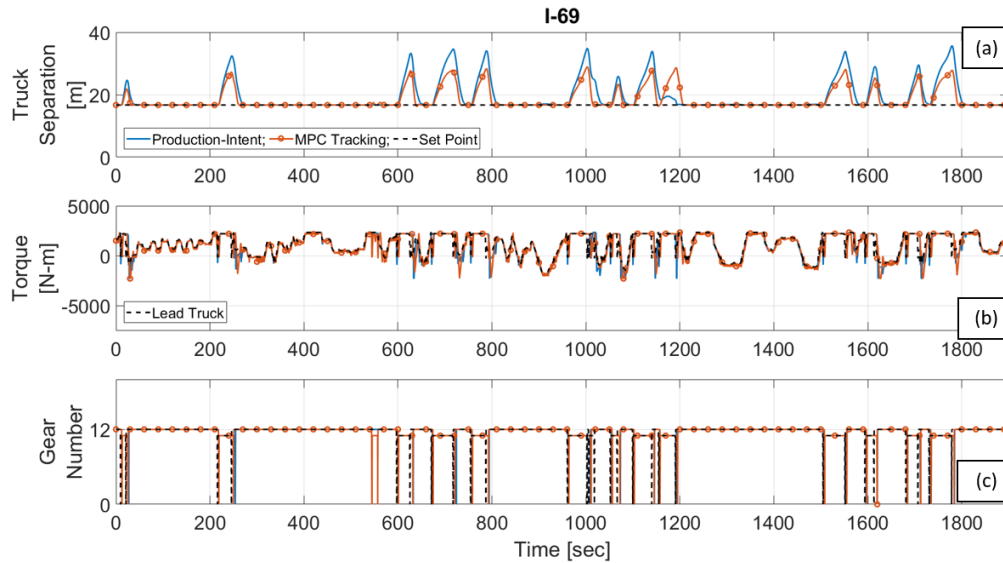


Fig. 4.5. A comparison of truck separation in meters (a), torque in Newton-meters (b), and gear number (c) between a production-intent controller and MPC over I-69.

MPC was able to reduce to some extent the distance the follow truck fell behind in many of these instances. An explanation for the reason why MPC performs better than the production-intent controller is shown in Figure 4.6.

When the platoon climbed the sustained uphill (Figure 4.6a), the lead truck downshifted (Figure 4.6b) and maxed out torque (Figure 4.6c), which caused an increase in relative velocity between the lead truck and the follow truck as shown in Figure 4.6d. This increase in relative velocity was further increased by the follow truck downshifting, which caused it to slow down even more. This increase in relative velocity between the two-trucks led to an increase in truck separation as shown in Figure 4.6e. The follow truck controlled by a production-intent controller decreased torque to match the lead truck when it downshifted to avoid encroaching, but this loss of momentum caused it to fall behind when it downshifted a few seconds later. The follow truck controlled by MPC knew that the lead truck would max out torque

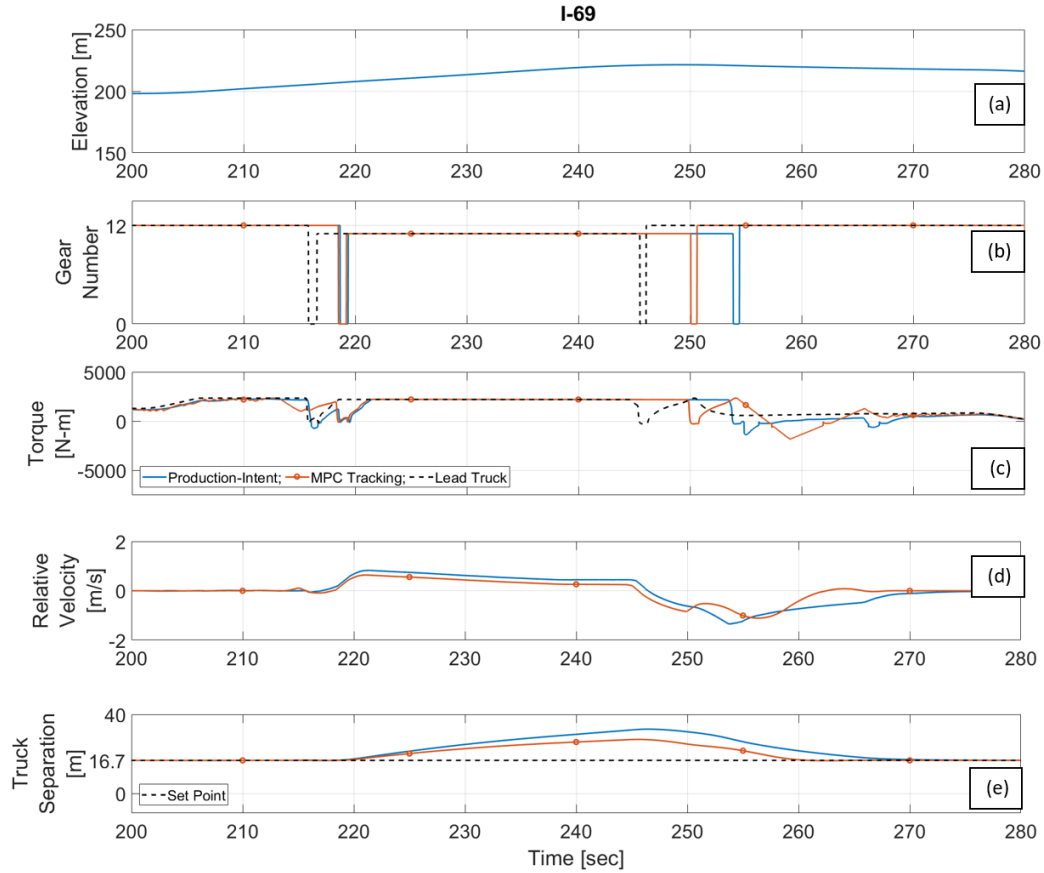


Fig. 4.6. Elevation in meters (a), gear number (b), engine torque in Newton-meters (c), relative velocity in meters per second (d), and truck separation in meters (e) is shown over I-69 between 200 and 280 seconds.

immediately after it shifted, so it kept its own torque at nearly maximum while the lead truck was downshifting. This slight increase in relative velocity for the follow truck controlled by MPC allowed it to fall behind less than the follow truck controlled by a production-intent controller.

Simultaneous shifting was applied to the follow truck controlled by a production-intent controller and the follow truck controlled by MPC to analyze the trade-off between simultaneous shifting and look-ahead knowledge. A comparison of the truck separation, torque, and gear number of the platoon with the follow truck controlled

by a production-intent controller and the platoon with the follow truck controlled by MPC with and without simultaneous shifting is shown in Figure 4.7 and a comparison of the tracking metrics is shown in Table 4.3.

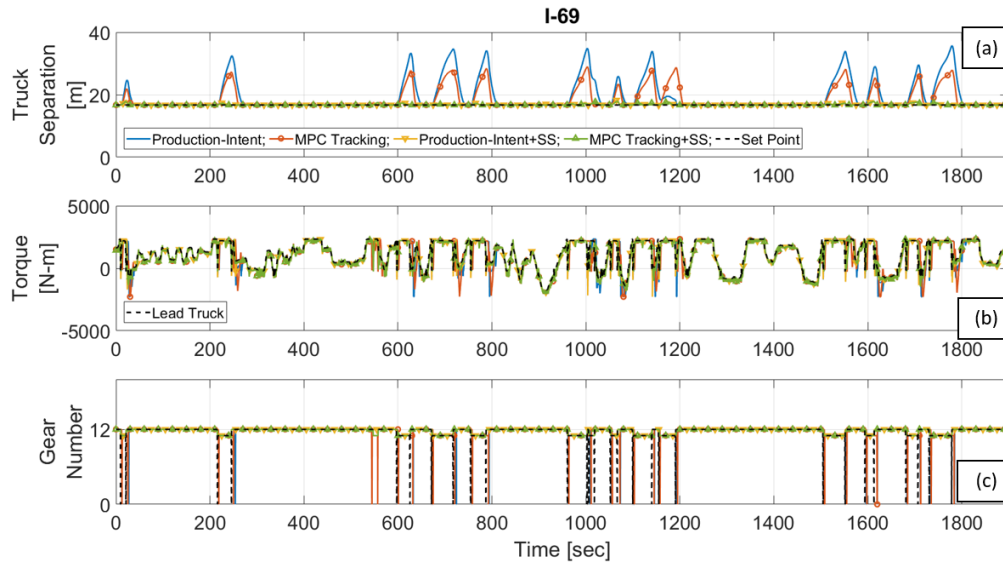


Fig. 4.7. A comparison of truck separation in meters (a), torque in Newton-meters (b), and gear number (c) between a production-intent controller and MPC with and without simultaneous shifting over I-69.

The significant improvement in tracking shown in Figure 4.7 and Table 4.3 by applying simultaneous shifting even without look-ahead knowledge demonstrates that sufficient tracking to platoon on routes with heavy grade can be largely realized by effective shifting strategies alone.

Table 4.3. Tracking metrics comparison between a production-intent controller and MPC with and without simultaneous shifting on I-69.

Strategy over I-69	Average Truck Separation (m)
Production-Intent	19.4
Production-Intent + Simultaneous Shifting	16.8
MPC	18.5
MPC + Simultaneous Shifting	16.8
Strategy over I-69	Maximum Truck Separation (m)
Production-Intent	35.8
Production-Intent + Simultaneous Shifting	18.5
MPC	29.0
MPC + Simultaneous Shifting	18.0

4.5 Fuel Consumption Comparison

A comparison of the fuel consumption between the platoon where the follow truck is controlled by a production-intent controller and the platoon where the follow truck is controlled by MPC on I-74 and the platoon where the follow truck is controlled by a production-intent controller and the platoon where the follow truck is controlled by MPC with and without simultaneous shifting on I-69 is shown in Table 4.4.

Neither MPC nor simultaneous shifting significantly affected the fuel consumption of the platoon because the drag coefficients of both trucks remained nearly unchanged even at the larger truck separations experienced momentarily over I-74 and I-69 when the follow truck is being controlled by a production-intent controller, as was shown in Figure 3.8.

Table 4.4. Fuel consumption comparison between a production-intent controller and MPC on I-74 and a production-intent controller and MPC with and without simultaneous shifting on I-69.

Strategy over I-74	Lead Truck Fuel Consumption
Single truck Baseline	1.0
Production-Intent	0.99
MPC	0.99
Strategy over I-74	Follow Truck Fuel Consumption
Single truck Baseline	1.0
Production-Intent	0.88
MPC	0.88
Strategy over I-69	Lead Truck Fuel Consumption
Single Truck Baseline	1.0
Production-Intent	0.99
Production-Intent + Simultaneous Shifting	0.99
MPC	0.99
MPC + Simultaneous Shifting	0.99
Strategy over I-69	Follow Truck Fuel Consumption
Single Truck Baseline	1.0
Production-Intent	0.95
Production-Intent + Simultaneous Shifting	0.93
MPC	0.95
MPC + Simultaneous Shifting	0.92

4.6 Summary

The follow truck's ability to successfully track the lead truck at the desired set point can be improved by leveraging look-ahead knowledge via model predictive control. However, simultaneous shifting strategies largely alleviated the need for look-ahead knowledge for the scenarios simulated for this thesis.

5. ROUTE OPTIMIZED GAP GROWTH TO MINIMIZE FUEL CONSUMPTION

5.1 Introduction

The previously described production-intent platooning controller minimizes fuel consumption for the platoon by having the follow truck attempt to maintain a fixed gap to reduce drag for both trucks. However, when the lead truck is being driven sub-optimally or when the grade is challenging enough, there are times when intentionally allowing the gap to increase can lead to increased fuel savings, as will be shown by this chapter. Implementation of such a strategy requires look-ahead knowledge of the lead truck's behavior and the upcoming grade over the route.

5.2 Route Optimized Gap Growth Framework and Algorithm Design

A linear model of a class 8 truck following another truck was developed for a Model Predictive Control (MPC) controller. The free body diagram of a class 8 truck shown in Figure 5.1 will be used as a reference for all of the forces on a semi truck.

The motive force on the truck was represented by:

$$F_{motive} = P_e/V \tag{5.1}$$

where P_e is engine power and V is velocity. Power was used because it is independent of gear number allowing the nonlinearities associated with gear shifting to be neglected within the controller. A similar equation was used to represent the brake force:

$$F_{brake} = P_{brake}/V \tag{5.2}$$

where P_{brake} is brake power and V is velocity.

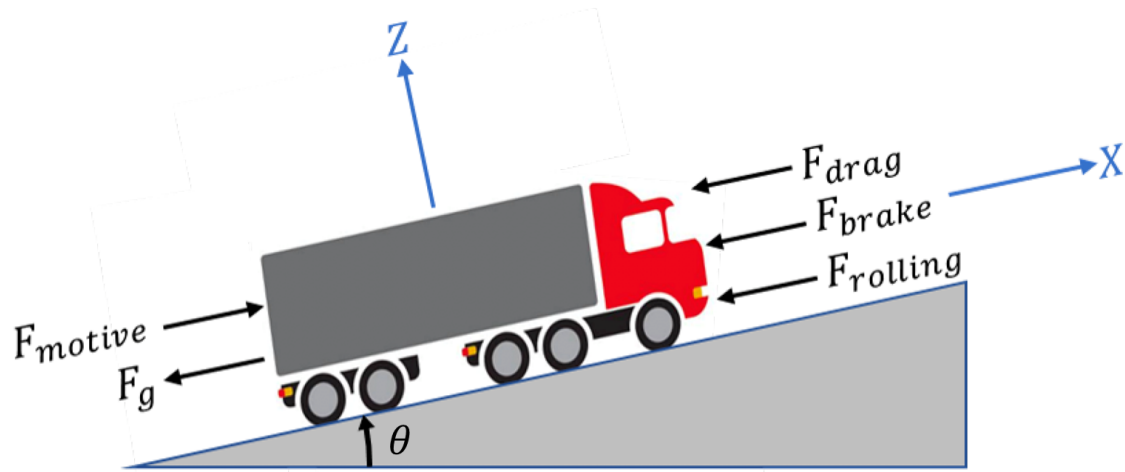


Fig. 5.1. A free-body diagram of forces acting on a class 8 truck.

The force of gravity was represented by:

$$F_{gravity} = mg\theta \quad (5.3)$$

where m is the mass of the truck, g is the gravity constant, and θ is grade. Small angle approximation was used to approximate $\sin(\theta)$ as θ .

The force of rolling resistance was represented by:

$$F_{roll} = mgf \quad (5.4)$$

where m is the mass of the truck, g is the gravity constant, and f is friction coefficient. Small angle approximation was used to approximate $\cos(\theta)$ as 1. The force of drag, which was mentioned earlier as varying with both velocity and truck separation, was represented by:

$$F_{drag} = 1/2\rho\bar{A}C_{D,0}(p_0V\bar{V} + p_1d\bar{V}^2) \quad (5.5)$$

where ρ is the density of air, $C_{D,0}$ is the nominal drag coefficient, V is the current velocity of the follow truck, \bar{V} is the average velocity of the follow truck over the

corridor, d is the distance between the lead truck and the follow truck, p_0 is the y-intercept of the linearization of drag as a function of distance for the follow truck, p_1 is the slope of the linearization of drag as a function of distance for the follow truck. This equation was obtained by linearizing the nonlinear drag variation as a function of truck separation shown in Figure 3.8. Then, a first-order Taylor expansion was applied to the force of drag to obtain its variation as a linear function of both velocity and truck separation.

Along with these forces, three coupling terms were considered: The difference between the trucks' current separation and the distance set point (which is 16.7 meters for platooning), the difference in velocity between the lead truck and the follow truck, and the distance between the lead truck and the follow truck. The difference between the current truck separation and the distance set point will be referred to as Δd in this thesis. The difference between the lead truck's velocity and the follow truck's will be referred to as ΔV . And, the distance between the lead truck and the follow truck will be referred to as d .

The prediction model for the system is shown below:

$$x[k + 1] = \mathbf{A}x[k] + \mathbf{B}u[k] + \mathbf{B}_a a[k] + \mathbf{B}_\theta \theta[k] \quad (5.6)$$

where x is the state vector, \mathbf{A} relates the evolution of states from one time instance to the next, u is the input vector, \mathbf{B} relates how the inputs affect the states, a is the lead vehicle's acceleration, \mathbf{B}_a relates how the lead vehicle's acceleration affects the states, θ is road grade, and \mathbf{B}_θ relates how the road grade affects the states. The acceleration of the lead truck and road grade were treated as disturbances so that they could change dynamically over the MPC horizon.

The state vector is shown below:

$$x = \begin{bmatrix} \Delta d \\ \Delta V \\ V \\ P_e \\ P_b \\ f \\ d \end{bmatrix} \quad (5.7)$$

where Δd is the distance between the platoon's current truck separation and the desired truck separation of 16.7 meters. ΔV is the relative velocity between the lead truck and the follow truck. V is the velocity of the follow truck. P_e is the engine power of the follow truck. P_b is the brake power of the follow truck. f is the friction coefficient. d is the distance between the lead truck and the follow truck.

The state matrix, \mathbf{A} , is shown below:

$$\mathbf{A} = \begin{bmatrix} 0 & 1 & 0 & 0 & 0 & 0 & 0 \\ 0 & 0 & \frac{\rho \bar{A} C_{D,0} \bar{V} p_0}{2m_e} & -\frac{\eta_t}{m_e \bar{V}} & \frac{1}{m_e \bar{V}} & \frac{m}{m_e} g & \frac{\rho \bar{A} C_{D,0} \bar{V}^2 p_1}{2m_e} \\ 0 & 0 & -\frac{\rho \bar{A} C_{D,0} \bar{V} p_0}{2m_e} & \frac{\eta_t}{m_e \bar{V}} & -\frac{1}{m_e \bar{V}} & -\frac{m}{m_e} g & -\frac{\rho \bar{A} C_{D,0} \bar{V}^2 p_1}{2m_e} \\ 0 & 0 & 0 & -\frac{1}{\tau_e} & 0 & 0 & 0 \\ 0 & 0 & 0 & 0 & -\frac{1}{\tau_b} & 0 & 0 \\ 0 & 0 & 0 & 0 & 0 & 0 & 0 \\ 0 & 1 & 0 & 0 & 0 & 0 & 0 \end{bmatrix} \quad (5.8)$$

where ρ is air density, \bar{A} is the frontal area of the semi truck, $C_{D,0}$ is the nominal drag coefficient, \bar{V} is the average velocity of the follow truck over the route, p_0 is the y-intercept of the linearization of drag as a function of distance for the follow truck, m_e is the inertial mass of the semi truck, η_t is the drivetrain efficiency, g is the gravity constant, p_1 is the slope of the linearization of drag as a function of distance for the follow truck, τ_e is the engine time constant, and τ_b is the brake time constant.

The input matrix, \mathbf{B} , is shown below:

$$\mathbf{B} = \begin{bmatrix} 0 & 0 \\ 0 & 0 \\ 0 & 0 \\ \frac{1}{\tau_e} & 0 \\ 0 & \frac{1}{\tau_b} \\ 0 & 0 \\ 0 & 0 \end{bmatrix} \quad (5.9)$$

where τ_e is the engine time constant, and τ_b is the brake time constant.

The acceleration input matrix, \mathbf{B}_a , is shown below:

$$\mathbf{B}_a = \begin{bmatrix} 0 \\ 1 \\ 0 \\ 0 \\ 0 \\ 0 \\ 0 \end{bmatrix} \quad (5.10)$$

The grade input matrix, \mathbf{B}_θ , is shown below:

$$\mathbf{B}_\theta = \begin{bmatrix} 0 \\ \frac{m}{m_e}g \\ -\frac{m}{m_e}g \\ 0 \\ 0 \\ 0 \\ 0 \end{bmatrix} \quad (5.11)$$

where m is the mass of the truck, g is the gravity constant, and m_e is the inertial mass.

The objective and constraints for the MPC, called Route Optimized Gap Growth (ROGG), are shown below:

$$\min J = \sum_{k=0}^{N-1} P_e[k]^2 \quad (5.12)$$

$$s.t. P_{e,min} \leq P_e \leq P_{e,max} \quad (5.13)$$

$$\dot{P}_{e,min} \leq \dot{P}_e \leq \dot{P}_{e,max} \quad (5.14)$$

$$0 \leq P_{brake} \leq P_{b,max} \quad (5.15)$$

$$d_{set} \leq d \leq d_{max} \quad (5.16)$$

where P_e is engine power, $P_{e,min}$ is maximum retarder (i.e. negative engine) power, $P_{e,max}$ is maximum positive engine power, \dot{P}_e is the rate of change of engine power, $\dot{P}_{e,min}$ is the fastest engine power can decrease, and $\dot{P}_{e,max}$ is the fastest engine power can increase, P_{brake} is brake power, $P_{b,max}$ is maximum brake power, d is the current truck separation, d_{set} is the set point distance for platooning, and d_{max} is the maximum allowed platooning distance. In short, the objective is to minimize power while maintaining realistic constraints on the engine, brakes, and truck separation.

The controller was applied to the entire route in open loop to generate an optimal truck separation, d_{des} , for the follow truck to platoon at.

5.3 Tracking MPC Framework and Algorithm Design

The tracking controller used in closed loop to follow the optimal truck separation trajectory had the same prediction model formulation, but it had a different objective

and constraints. The objective and constraints for the tracking MPC controller are shown below:

$$\min J = \sum_{k=0}^{N-1} (d[k] - d_{des}[k])^2 \quad (5.17)$$

$$s.t. P_{e,min} \leq P_e \leq P_{e,max} \quad (5.18)$$

$$\dot{P}_{e,min} \leq \dot{P}_e \leq \dot{P}_{e,max} \quad (5.19)$$

$$0 \leq P_{brake} \leq P_{b,max} \quad (5.20)$$

$$(5.21)$$

where d is the distance between the lead truck and the follow truck, d_{des} is the desired truck separation calculated by the ROGG controller, P_e is engine power, $P_{e,min}$ is maximum retarder power, $P_{e,max}$ is maximum positive engine power, \dot{P}_e is the rate of change of engine power, $\dot{P}_{e,min}$ is the fastest engine power can decrease, and $\dot{P}_{e,max}$ is the fastest engine power can increase P_{brake} , is brake power, and $P_{b,max}$ is maximum brake power. In short, the objective is to minimize tracking error while maintaining realistic constraints on the engine and brakes.

The tracking controller was applied with a 15-second look-ahead horizon in closed loop with the vehicle models and driver model described in chapter 3.

A summary of the implementation of ROGG with the tracking controller is shown in Figure 5.2.

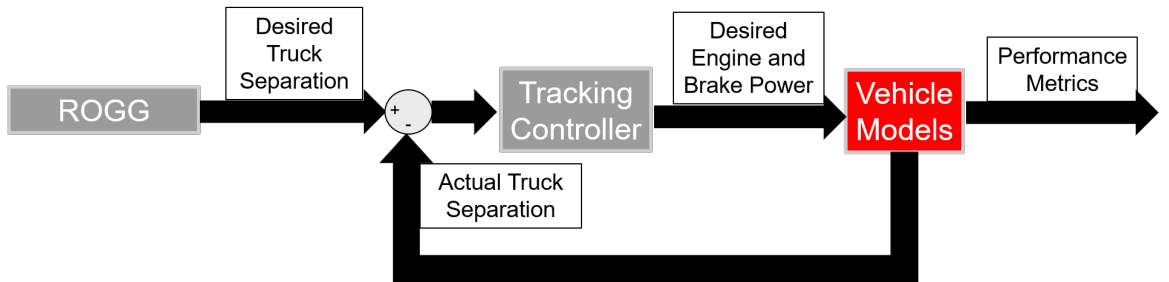


Fig. 5.2. Diagram of Route Optimized Gap Growth implementation

ROGG calculates the desired truck separation for a given route and provides that information to the tracking controller. The tracking controller then calculates the desired engine and brake power to follow the lead truck at the desired truck separation. The vehicle models feed back into the tracking controller the actual truck separation that resulted from implementing the desired control inputs and generate important performance metrics such as fuel consumption.

5.4 Westbound I-74 in Indiana (Moderate Grade)

The first route used for analysis was the moderately challenging grade route of I-74 with a constant velocity set point of 29 m/s shown in Figure 5.3.

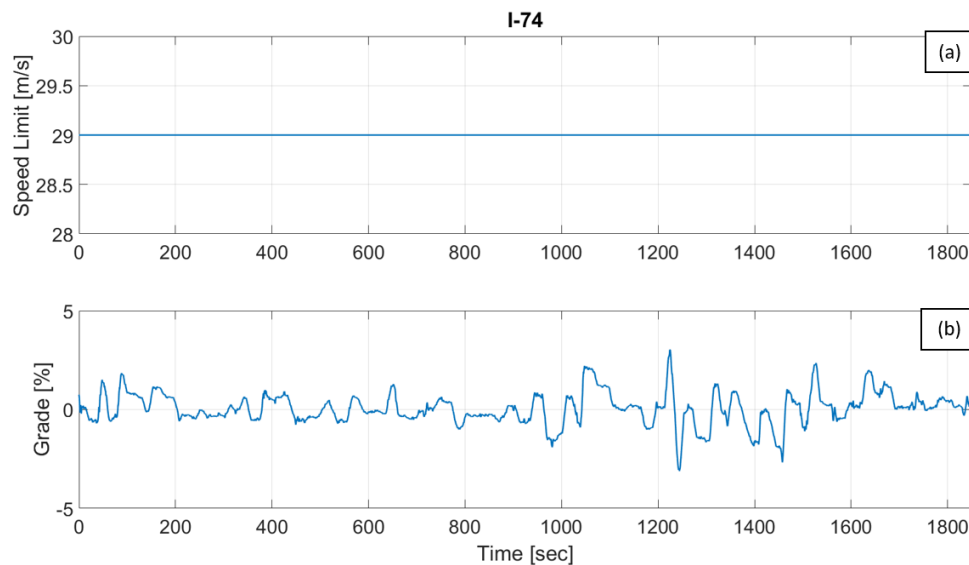


Fig. 5.3. Constant velocity data for westbound I-74 (a) time aligned with grade data for the route (b).

A comparison of the desired truck separation calculated by ROGG over I-74 and the actual truck separation the tracking MPC controller was able to achieve is shown in Figure 5.4.

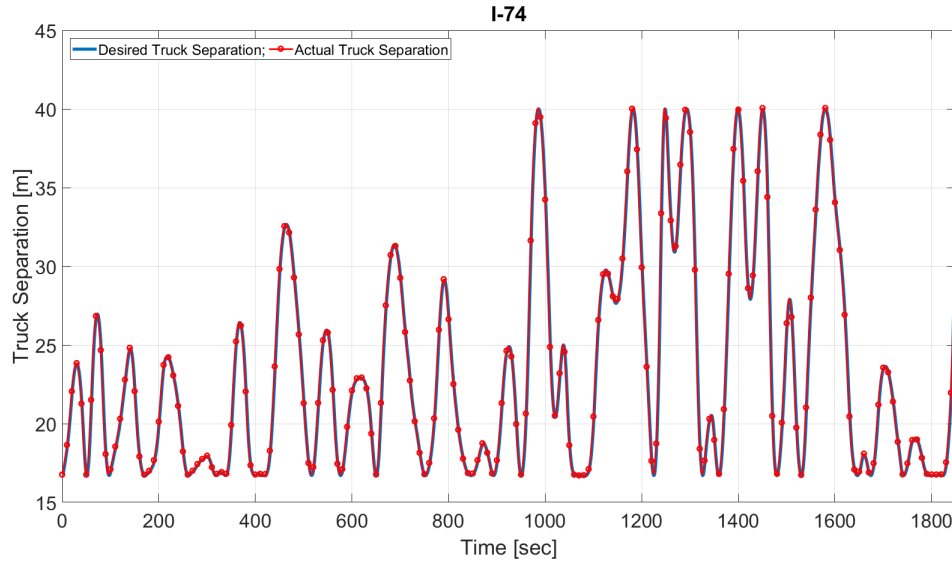


Fig. 5.4. Comparison of desired truck separation and actual truck separation over I-74.

Figure 5.4 shows that the tracking MPC controller was able to effectively track the desired trajectory over I-74. Figure 5.5 compares the truck separation and torque of the platoon with the follow truck controlled by a production-intent controller and the platoon with the follow truck controlled by ROGG with a maximum allowed truck separation of 40 meters. Table 5.1 compares the fuel consumption between the two strategies.

ROGG allowed the follow truck to save an extra percent of fuel when compared to a production-intent controller, and the lead truck consumed approximately the same amount of fuel, so the platoon was able to save an extra half-percent of fuel. As shown in 5.5b, ROGG saves fuel by reducing how aggressively the follow truck's torque changes and reducing the amount of time the follow truck spends at maximum torque. However, the follow truck commanded by a production-intent controller did not saturate frequently over this moderately challenging grade route, and its torque

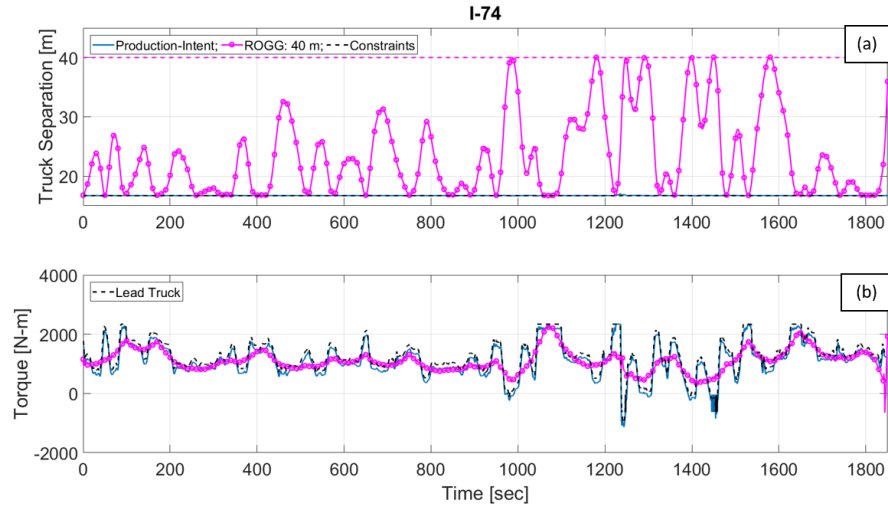


Fig. 5.5. Comparison of truck separation (a) and torque (b) for a production-intent controller and ROGG up to 40 meters over I-74.

Table 5.1. Fuel consumption comparison between a production-intent controller and ROGG up to 40 meters on I-74.

Strategy over I-74	Lead Truck Fuel Consumption
Single Truck Baseline	1.0
Production-Intent	0.99
ROGG: 40 m	0.99
Strategy over I-74	Follow Truck Fuel Consumption
Single Truck Baseline	1.0
Production-Intent	0.88
ROGG: 40 m	0.87

commands were not very aggressive, so there was little room for improvement using ROGG.

The maximum truck separation allowed for ROGG was reduced from 40 meters, to 30 meters, and then to 25 meters to see how much reducing the maximum allowed truck separation would decrease the obtained fuel savings. A comparison of fuel consumption is shown in Table 5.2, and a comparison of the truck separation and torque of the platoon with the follow truck controlled by a production-intent controller and the platoon with the follow truck controlled by ROGG at various allowed maximum truck separations is shown in Figure 5.6.

Table 5.2. Fuel consumption comparison between a production-intent controller and ROGG up to 40 meters, 30 meters, and 25 meters on I-74.

Strategy over I-74	Lead Truck Fuel Consumption
Single Truck Baseline	1.0
Production-Intent	0.99
ROGG: 40 m	0.99
ROGG: 30 m	0.99
ROGG: 25 m	0.99
Strategy over I-74	Follow Truck Fuel Consumption
Single Truck Baseline	1.0
Production-Intent	0.88
ROGG: 40 m	0.87
ROGG: 30 m	0.87
ROGG: 25 m	0.87

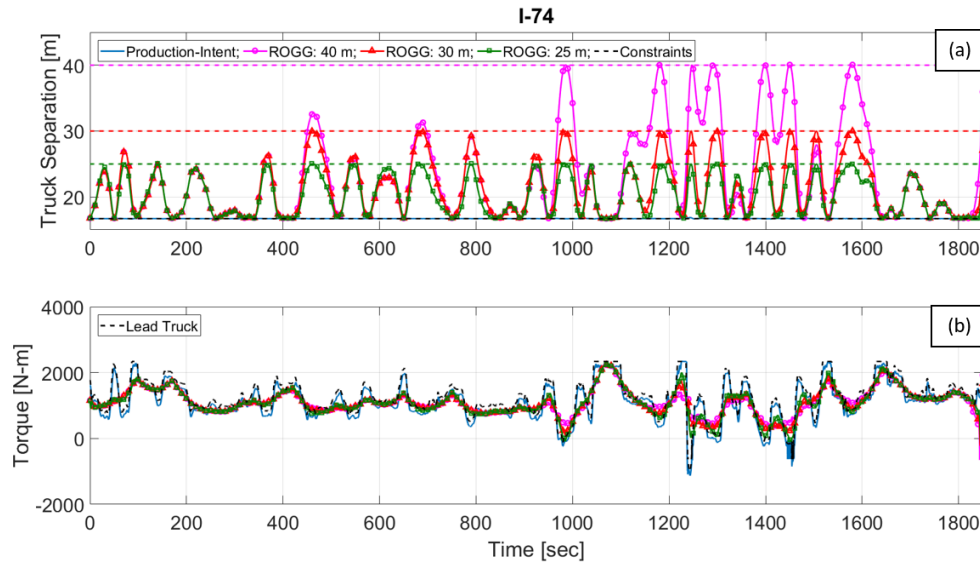


Fig. 5.6. Comparison of truck separation (a) and torque (b) for a production-intent controller and ROGG up to 40 meters, 30 meters, and 25 meters over I-74.

The fuel consumption remains approximately the same even as the maximum allowed truck separation decreased, as can be seen in Figure 5.7, because the grade over I-74 was not varying aggressively enough.

The standard deviation of 5 km of grade (2.5 kilometers to the left and 2.5 kilometers to the right of the given position on the corridor) was taken as a metric for how aggressive grade variation was over a route. The grade and the standard deviation of 5 km of grade over I-74 is shown in Figure 5.8.

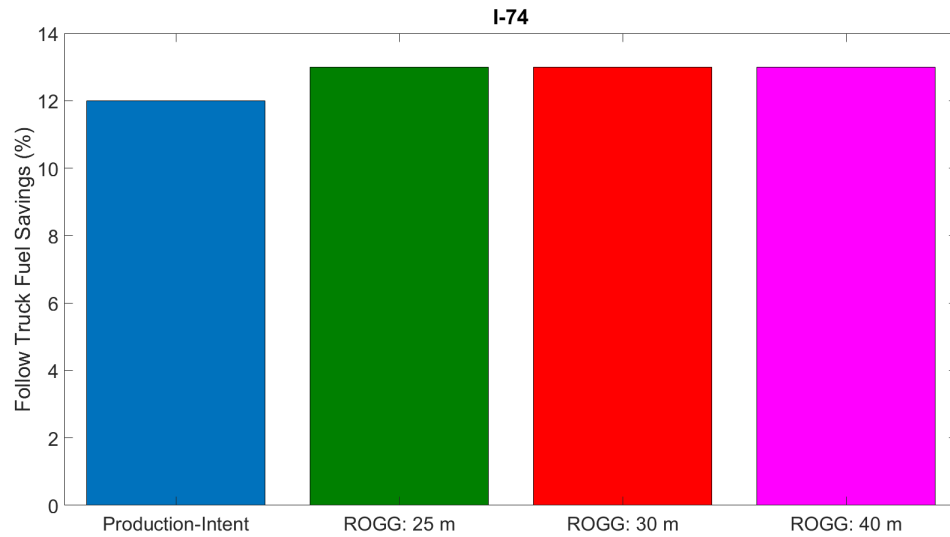


Fig. 5.7. Comparison of fuel savings for the follow truck as a function of maximum allowed truck separation for ROGG and a production-intent controller with a set point of 16.7 meters.

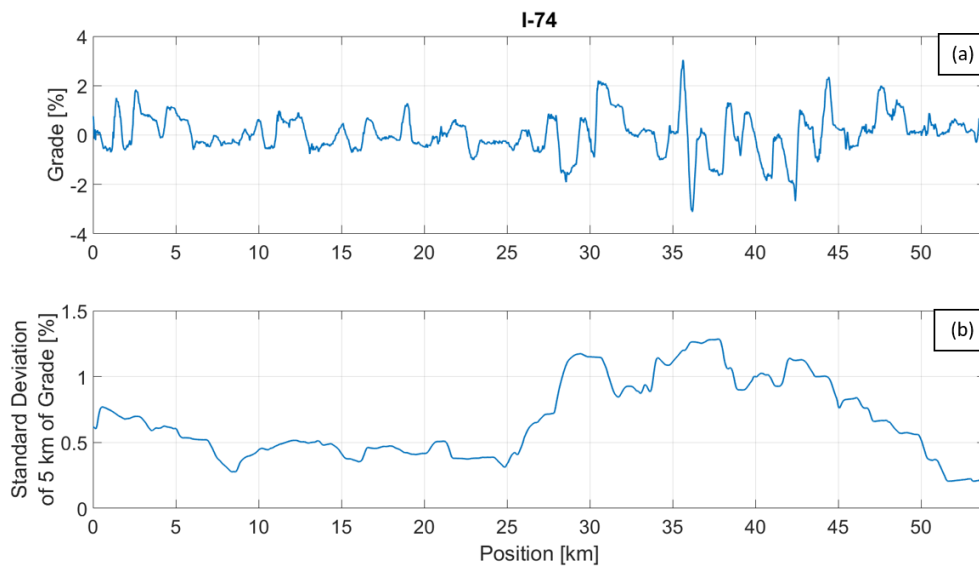


Fig. 5.8. Grade (a) and standard deviation of 5 km of grade (b) over I-74.

The more aggressive the grade variation, the more the extra truck separation allowed by ROGG at larger distances can be leveraged to use smoother torque commands and saturate less frequently. Analysis of ROGG over various routes revealed that there is only a significant fuel savings benefit to ROGG when compared to a production-intent controller when the standard deviation of 5 km of grade surpasses approximately 1.5%, and this benefit increases as the maximum allowed truck separation increases. Over I-74, a standard deviation of 5 km of grade of 1.5% was never reached.

5.5 Northbound I-69 in Indiana (Heavy Grade)

A more challenging grade route, I-69 with a constant velocity set point of 27.5 m/s is shown in Figure 5.9 and is considered next.

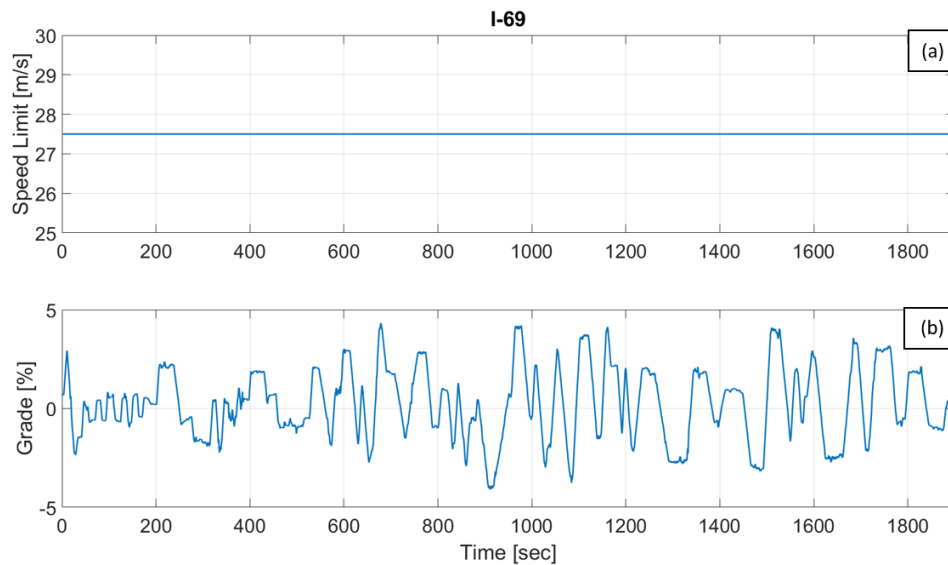


Fig. 5.9. Constant velocity data for northbound I-69 (a) time aligned with grade data for the route (b).

As shown in Figure 5.10, The tracking MPC controller had more of a challenge tracking the desired truck separation on I-69 compared to I-74 because the route had greater grade variation, but the controller still successfully tracked the desired trajectory for most of the route.

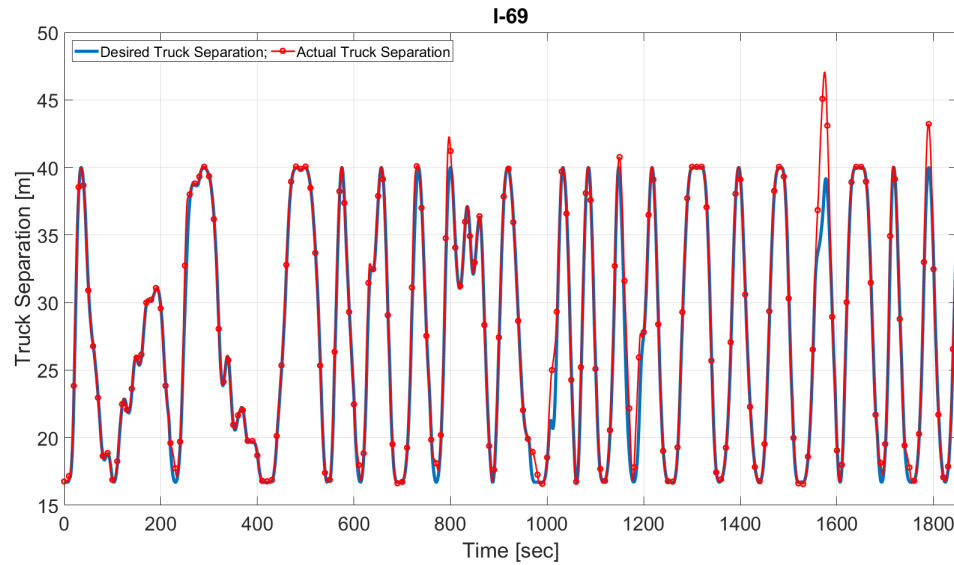


Fig. 5.10. Comparison of desired truck separation and actual truck separation over I-69.

Figure 5.11 compares the truck separation and torque of the platoon with the follow truck controlled by a production-intent controller and the platoon with the follow truck controlled by ROGG with a maximum allowed truck separation of 40 meters. Table 5.3 compares the fuel consumption between the two strategies.

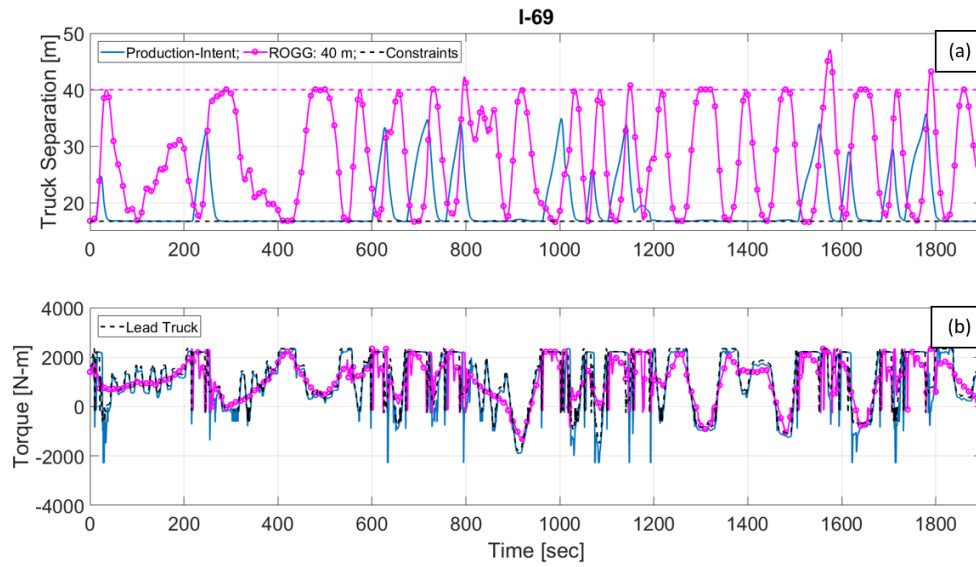


Fig. 5.11. Comparison of truck separation (a) and torque (b) for a production-intent controller and ROGG up to 40 meters over I-69.

Table 5.3. Fuel consumption comparison between a production-intent controller and ROGG up to 40 meters on I-69.

Strategy over I-69	Lead Truck Fuel Consumption
Single Truck Baseline	1.0
Production-Intent	0.99
ROGG: 40 m	0.99
Strategy over I-74	Follow Truck Fuel Consumption
Single Truck Baseline	1.0
Production-Intent	0.95
ROGG: 40 m	0.88

Over this more challenging route, ROGG allowed the follow truck to save a significant amount of fuel by reducing how aggressively the follow truck's torque changed and by decreasing the amount of time the follow truck spent at maximum torque. The lead truck consumed slightly more fuel because of the increase in drag it experienced when the follow truck was platooning at a further distance than the set point, but the platoon-average fuel consumption was reduced by an additional 3% when compared to a production-intent controller.

The maximum truck separation allowed for ROGG was reduced to 30 meters then to 25 meters, to see how much reducing the maximum allowed truck separation would decrease the obtained fuel savings. A comparison of the truck separation and torque of the platoon with the follow truck controlled by a production-intent controller and the platoon with the follow truck controlled by ROGG up to 40 m, 30 m, and 25 m is shown in Figure 5.12, and a comparison of the fuel consumption of the various strategies is shown in Table 5.4.

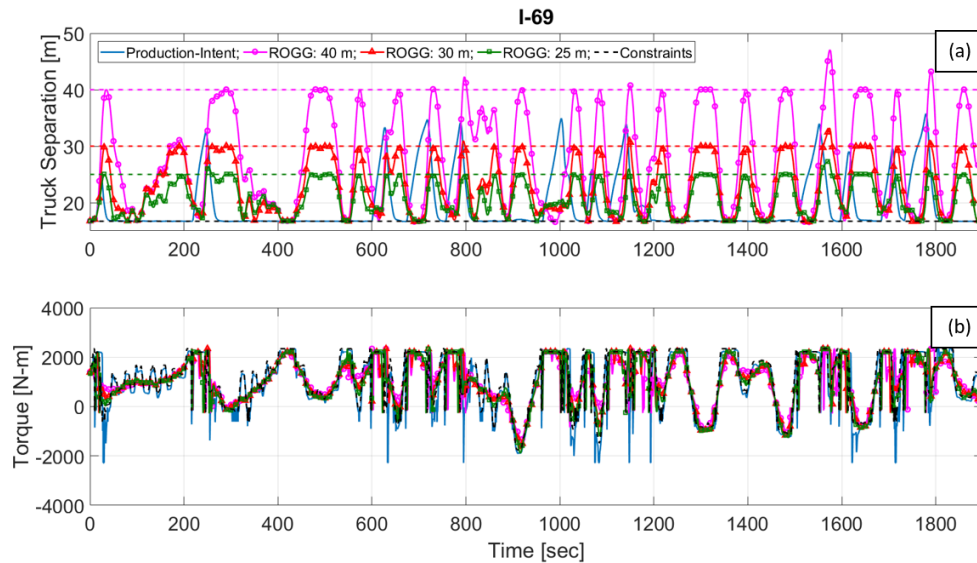


Fig. 5.12. Comparison of truck separation (a) and torque (b) for a production-intent controller and ROGG up to 40 meters, 30 meters, and 25 meters over I-69.

Table 5.4. Fuel consumption comparison between a production-intent controller and ROGG up to 40 meters, 30 meters, and 25 meters on I-69.

Strategy over I-69	Lead Truck Fuel Consumption
Single Truck Baseline	1.0
Production-Intent	0.99
ROGG: 40 m	0.99
ROGG: 30 m	0.99
ROGG: 25 m	0.99
Strategy over I-69	Follow Truck Fuel Consumption
Single Truck Baseline	1.0
Production-Intent	0.95
ROGG: 40 m	0.88
ROGG: 30 m	0.88
ROGG: 25 m	0.89

As was stated in the previous section, the more aggressive the grade variation, the more a larger maximum distance is beneficial to ROGG. The grade and the standard deviation of 5 km of grade over I-69 is shown in Figure 5.13.

About a third of the way through I-69, the standard deviation of 5 km of grade surpassed 1.5% and remained above that value for most of the rest of the route, so ROGG showed a significant benefit over this route by allowing the follow truck to use smoother torque commands and saturate less frequently. The increasing benefit of ROGG as a function of truck separation is shown in Figure 5.14.

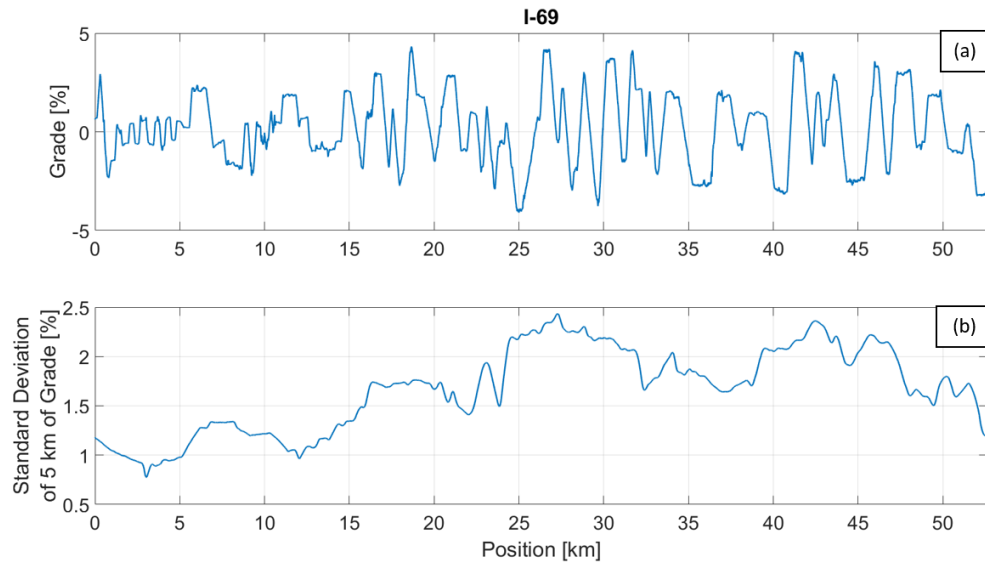


Fig. 5.13. Grade (a) and standard deviation of 5 km of grade (b) over I-69.

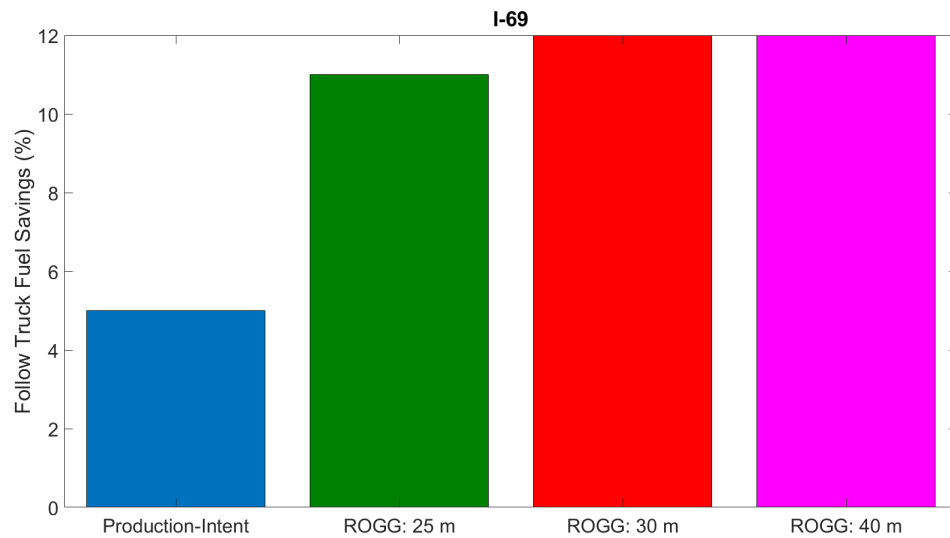


Fig. 5.14. Comparison of fuel savings for the follow truck as a function of maximum allowed truck separation for ROGG and a production-intent controller with a set point of 16.7 meters.

5.6 Summary

Changing the desired truck separation based on look-ahead knowledge slightly increased fuel savings on moderately challenging grade routes. This slight increase in fuel savings was not sensitive to the maximum allowed truck separation. However, on heavy grade routes, ROGG significantly increased fuel savings by decreasing the amount of time the follow truck spent saturating torque and by decreasing how aggressively the follow truck varied torque, and a larger allowed maximum truck separation played a significant role in how much fuel savings could be obtained with ROGG.

6. SUMMARY AND FUTURE WORK

This thesis analyzed strategies to improve the tracking and fuel savings of platooning over routes with moderate grade and heavy grade. The first strategy that was analyzed was simultaneous shifting, having the follow truck shift at the same time as the lead truck unless shifting will cause its engine to overspeed or underspeed. Simultaneous shifting showed tremendous value in improving tracking over challenging grade routes, and, consequently, improving driver comfort. It did not affect fuel consumption directly, but will enable safe platooning over more routes with challenging grade. Therefore, the fuel savings of platooning can be realized on a greater number of routes.

The second strategy that was analyzed was leveraging look-ahead knowledge to improve tracking on moderate and heavy grade routes through model predictive control. A production-intent platooning controller was capable of maintaining the desired set point without look-ahead knowledge on a route with moderately challenging grade; however, look-ahead knowledge did improve tracking on a route with heavy grade. The value of look-ahead knowledge from a tracking perspective was largely alleviated by simultaneous shifting.

Lastly, look-ahead knowledge was utilized to improve fuel consumption for the follow truck by intentionally allowing the truck separation to increase at optimal instances during the route based on the upcoming grade and the lead truck's acceleration via a Model Predictive Control (MPC) strategy called Route Optimized Gap Growth (ROGG). ROGG demonstrated slight fuel savings on a moderately challenging grade route and significant fuel savings on a route with heavy grade. On the route with heavy grade, these fuel savings increased as the maximum allowed truck separation increased.

The next step for model predictive control is to extend its application from just the follow truck in the platoon to simultaneous control of both trucks in a platoon. Strategies optimized to reduce fuel consumption for a single truck have been developed for the research project, and strategies optimized to reduce fuel consumption for the follow truck in a platoon, such as ROGG, have been developed as well, but a strategy that minimizes fuel consumption for both trucks simultaneously should enable the highest fuel savings.

The results shown in this paper were only shown for a high-fidelity simulation. As a part of the research project, the strategies detailed in this paper will be verified on an engine test bed and on instrumented semi trucks. The torque and speed profiles generated by the simulation framework will be tested on an engine test bed to verify that the fuel savings obtained in simulation are realistic and the torque and speed commands are implementable. Then, the strategies tested in simulation will be executed on instrumented semi trucks on the trucking corridors mentioned in this thesis to verify that the fuel savings predicted in simulation can be realized in the real world.

7. OTHER CONTRIBUTIONS

The simulation and algorithm development described in this thesis is only a portion of a larger project to realize significant fuel savings on semi trucks. The torque and speed profiles generated by the algorithms run on the simulation framework described in this thesis will be tested on an engine test bed, shown in Figure 7.1, to verify the fuel savings predicted in simulation.



Fig. 7.1. Cummins X15 engine test bed in Herrick Laboratories at Purdue University.

Lastly, the algorithms implemented in simulation will be tested on class 8 trucks, such as the ones shown in Figure 7.2, to verify that the fuel savings predicted in simulation can be obtained in real-world scenarios.

Along these lines, the author contributed in several ways to the NEXTCAR project that were not included in this thesis by:

1. Developing a wiring diagram for the front panel of the engine test bed mentioned in the introduction of this thesis. The front panel includes the key switch, oil gauge, engine bypass, emergency stop, and various other important components. Once the



Fig. 7.2. Class 8 trucks representative of the trucks that will be used to verify the algorithms developed for the NEXTCAR project.

wiring diagram was completed, the front panel was constructed and is currently being used for engine testing.

2. Constructing an aftertreatment system for the engine test bed. A Computer-Aided Design (CAD) model was created of the engine test cell. Then, the aftertreatment was designed to meet several requirements on length and functionality. Once designed, the aftertreatment system was machined and constructed and is currently being used for engine testing.

3. Designing and constructing the thermocouple system that is currently being used for engine testing.

4. Enabling real-time Transmission Control Protocol (TCP) communication between a real-time target machine and a computer that controlled the test cell's dynamometer. Real-time communication was established to enable Hardware-In-the-Loop (HIL) testing of algorithm strategies.

5. Incorporating Dynamic Programming (DP) speed profiles calculated to optimize fuel savings for a single truck into the simulation framework and verifying the fuel savings for a single truck and for a platoon over various routes. Detailed analysis on where the fuel savings were coming from when compared to a single truck

traversing the same corridor while attempting to maintain a constant velocity was also obtained.

6. Implementing a Model Predictive Control (MPC) strategy to reduce fuel consumption on a short horizon in closed loop to analyze the trade-off between short horizon prediction with feedback compared with the long horizon results demonstrated by ROGG in this thesis.

7. Developing a MPC strategy to generate a velocity profile that will optimize fuel consumption for a single truck over an entire route without increasing trip time then extending the optimization to generate a velocity profile for the lead truck and the truck separation for the follow truck in a platoon that will optimize fuel consumption.

REFERENCES

REFERENCES

- [1] F. H. Administration. (2016) Highway statistics 2016. [Online]. Available: <https://afdc.energy.gov/data/10309>
- [2] INDOT. (2014) Indiana multimodal freight and mobility plan. [Online]. Available: https://www.in.gov/indot/files/2014_FP_Final.pdf
- [3] M. A. S. Kamal, M. Mukai, J. Murata, and T. Kawabe, “Model predictive control of vehicles on urban roads for improved fuel economy,” *IEEE Transactions on Control Systems Technology*, vol. 21, no. 3, pp. 831–841, May 2013.
- [4] S. Li, K. Li, R. Rajamani, and J. Wang, “Model predictive multi-objective vehicular adaptive cruise control,” *IEEE Transactions on Control Systems Technology*, vol. 19, no. 3, pp. 556–566, May 2011.
- [5] S. Xu, S. E. Li, B. Cheng, and K. Li, “Instantaneous feedback control for a fuel-prioritized vehicle cruising system on highways with a varying slope,” *IEEE Transactions on Intelligent Transportation Systems*, vol. 18, no. 5, pp. 1210–1220, May 2017.
- [6] A. Alam, J. Mrtensson, and K. H. Johansson, “Experimental evaluation of decentralized cooperative cruise control for heavy-duty vehicle platooning,” vol. 38, no. Complete, pp. 11–25, 2015.
- [7] B. Nemeth and P. Gspr, “Road inclinations in the design of lqv-based adaptive cruise control,” *IFAC Proceedings Volumes (IFAC-PapersOnline)*, vol. 18, 08 2011.
- [8] L. Bertoni, J. Guanetti, M. Basso, M. Masoero, S. Cetinkunt, and B. Francesco.
- [9] B. Sakhdari, E. M. Shahrivar, and N. L. Azad, “Robust tube-based mpc for automotive adaptive cruise control design,” in *2017 IEEE 20th International Conference on Intelligent Transportation Systems (ITSC)*, Oct 2017, pp. 1–6.
- [10] S. E. Li, Q. Guo, S. Xu, J. Duan, S. Li, C. Li, and K. Su, “Performance enhanced predictive control for adaptive cruise control system considering road elevation information,” *IEEE Transactions on Intelligent Vehicles*, vol. 2, no. 3, pp. 150–160, Sep. 2017.
- [11] V. Turri, B. Besselink, and J. K. H., “Cooperative look-ahead control for fuel-efficient and safe heavy-duty vehicle platooning,” *IEEE*, pp. 12–27.
- [12] T. Stanger and L. del Re, “A model predictive cooperative adaptive cruise control approach,” *American Control Conference*, pp. 1374–1379, 2013.

- [13] A. Kaku, A. S. Kamal, M. Mukal, and T. Kawabe, “Model predictive control for ecological vehicle synchronized driving considering varying aerodynamic drag and road shape information,” *SICE Journal of Control, Measurement, and System Integration*, pp. 299–308, 2013.
- [14] K. Yu, H. Yang, X. Tan, T. Kawabe, Y. Guo, Q. Liang, Z. Fu, and Z. Zheng, “Model predictive control for hybrid electric vehicle platooning using slope information,” *IEEE Transactions on Intelligent Transportation Systems*, vol. 17, no. 7, pp. 1894–1909, July 2016.
- [15] O. Santin, J. Pekar, J. Beran, A. D’Amato, J. Michelini, S. Szwabowski, and D. Filev, “Cruise controller with fuel optimization based on adaptive nonlinear predictive control,” *SAE Tech. Pap. 2016-01-0155*, pp. 1–13, 2016.
- [16] J. Gorzelany. (2018) Pros and cons of continuously variable transmissions. [Online]. Available: <https://www.carfax.com/blog/CVT-pros-and-cons>
- [17] D. Corona and B. De Schutter, “Adaptive cruise control for a smart car: A comparison benchmark for mpc-pwa control methods,” *IEEE Transactions on Control Systems Technology*, vol. 16, no. 2, pp. 365–372, March 2008.
- [18] Q. Xin, *Diesel Engine System Design*, ser. Woodhead Publishing in mechanical engineering. Elsevier Science, 2011. [Online]. Available: https://books.google.com/books?id=_HZwAgAAQBAJ
- [19] R. C. Services. (2019) How better aerodynamics lead to fuel savings. [Online]. Available: <https://www.rtscarrierservices.com/article/how-better-aerodynamics-lead-fuel-savings>
- [20] H. A. C. M. T. L. Bradley, Stephen P., *Applied Mathematical Programming*. Addison-Wesley, 1977.
- [21] E. Ozatay, S. Onori, J. Wollaeger, U. Ozguner, G. Rizzoni, D. Filev, J. Michelini, and S. Di Cairano, “Cloud-based velocity profile optimization for everyday driving: A dynamic-programming-based solution,” *IEEE Transactions on Intelligent Transportation Systems*, vol. 15, no. 6, pp. 2491–2505, Dec 2014.
- [22] E. Hellstrm, M. Ivarsson, J. slund, and L. Nielsen, “Look-ahead control for heavy trucks to minimize trip time and fuel consumption,” *Control Engineering Practice*, vol. 17, no. 2, pp. 245 – 254, 2009. [Online]. Available: <http://www.sciencedirect.com/science/article/pii/S0967066108001251>
- [23] D. Shen, D. Karbowski, and A. Rousseau, “Fuel efficient speed optimization for real-world highway cruising,” in *WCX World Congress Experience*. SAE International, apr 2018. [Online]. Available: <https://doi.org/10.4271/2018-01-0589>
- [24] B. Groelke, J. Borek, C. Earnhardt, J. Li, S. Geyer, and C. Vermillion, “A comparative assessment of economic model predictive control strategies for fuel economy optimization of heavy-duty trucks,” in *2018 Annual American Control Conference (ACC)*, June 2018, pp. 834–839.
- [25] T. B. Blog. (2017) Why were investing in the future of transportation and fuel efficiency. [Online]. Available: <https://www.breakthroughfuel.com/blog/peloton-future-transportation/>

- [26] B. Kouvaritakis and M. Cannon, *Model Predictive Control: Classical, Robust and Stochastic*, ser. Advanced Textbooks in Control and Signal Processing. Springer International Publishing, 2015. [Online]. Available: <https://books.google.com/books?id=DmoiCwAAQBAJ>
- [27] B. W. Bequette. (2009) Model predictive control: An overview and selected applications. [Online]. Available: <https://www.aiche.org/academy/webinars/model-predictive-control-overview-and-selected-applications>
- [28] J. H. Lee. (2005) A lecture on model predictive control. [Online]. Available: <http://cepac.cheme.cmu.edu/pasilectures/lee/LecturenoteonMPC-JHL.pdf>
- [29] A. H. Taylor, M. J. Droege, G. M. Shaver, J. A. Sandoval, S. Erlien, and J. Kuszmaul, "Capturing the impact of speed, grade, and traffic on class 8 truck platooning," *TBD*, pp. 1–13, 2018.
- [30] K. Salari, "DOE's Effort to Improve Heavy Vehicle Fuel Efficiency through Improved Aerodynamics Overview: LLNL-PRES-688057," U.S. Department of Energy by Lawrence Livermore National Laboratory, Washington, D.C., Tech. Rep.
- [31] M. Roeth, Switkes, and Josh, "Peloton technology platooning test," NACFE, Tech. Rep., 2013.